

Evolution of MHD Instabilities and its Stabilization in Tokamak Plasmas

Riaz Khan and N. Mizuguchi

-
- 1) National Tokamak Fusion Program, PAKISTAN**
 - 2) National Institute for Fusion Science, Toki, Japan**
-

5th IAEA Technical Meeting on Theory of Plasma Instabilities

September 5-10, 2011, Austin, Texas

Outline of Talk

- **Introduction**
- **Experimental Observation (MAST, NSTX)**
- **Simulation Model**
- **Simulation Results**
- **Conclusion**

Introduction

- MHD is derived from *magneto*- meaning magnetic field, and *hydro*- meaning fluid, and dynamics meaning movement
- The idea of MHD is that magnetic fields can induce currents in a moving conductive fluid, which create forces on the fluid, and also change the magnetic field itself.
- The MHD model is a combination of Maxwell's equations with the equations of gas dynamics and equations describing the interaction of the conductive fluid with the magnetic fields

Magnetohydrodynamics

- (mass)Density conservation: $\frac{\partial \rho}{\partial t} = -\nabla \cdot (\rho \mathbf{v})$
- Momentum conservation: $\rho \frac{\partial \mathbf{v}}{\partial t} = -\rho \mathbf{v} \cdot \nabla \mathbf{v} - \nabla p + \frac{1}{\mu_0} \mathbf{J} \times \mathbf{B}$
- Energy conservation: $\frac{\partial p}{\partial t} = -\mathbf{v} \cdot \nabla p - \gamma p \nabla \cdot \mathbf{v}$
- Faraday: $\frac{\partial \mathbf{B}}{\partial t} = -\nabla \times \mathbf{E}$
- Ohm's Law: $\mathbf{E} = -\mathbf{v} \times \mathbf{B} + \eta \mathbf{J}$
- Absence of magnetic charges $\nabla \cdot \mathbf{B} = 0$

These equations are solved to investigate a plasma equilibrium and the stability of this equilibrium to perturbations.

Characteristics of MHD activities

MHD instabilities play Important roles in fusion expt.

Negative

- **limit accessible operating regime,**
- **restrict the fusion output,**
- **minimize power plant size**

Positive

- **achieve quasi-stationary discharge conditions,**
- **limit the impurity accumulation in the plasma**

An MHD instability is characterized by:

- **mode numbers (m, n) (helicity of the instability)**
- **mode frequency (ω) (the rotation frequency of the instability)**
- **growth rate (γ) (growth and decay of instability)**
- **radial structure of the displacement eigen function (ξ)**

Types of MHD Instabilities

Driving forces for ideal (no dissipation) MHD instabilities:

- Pressure gradient (i.e. Ballooning Instability)
- Parallel current density (i.e. Kink mode)

Ballooning Instability:

- Pressure gradient (∇p) against curvature (κ)
- Unstable on outside of torus, stabilizing on inside
- Localized on low-field (outer-side) of torus
- High toroidal mode numbers most unstable

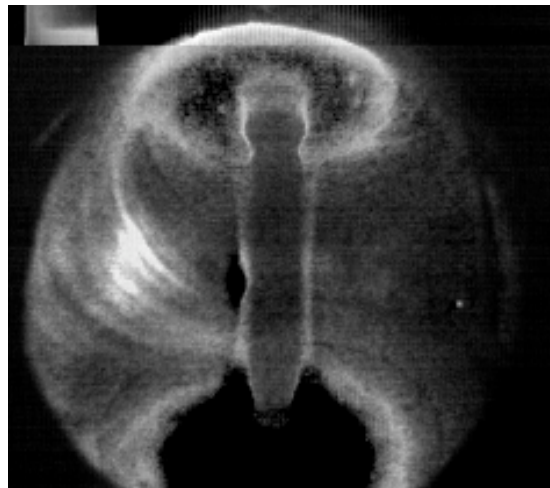
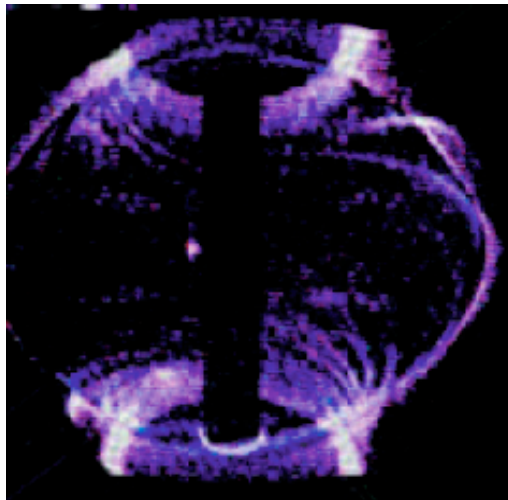
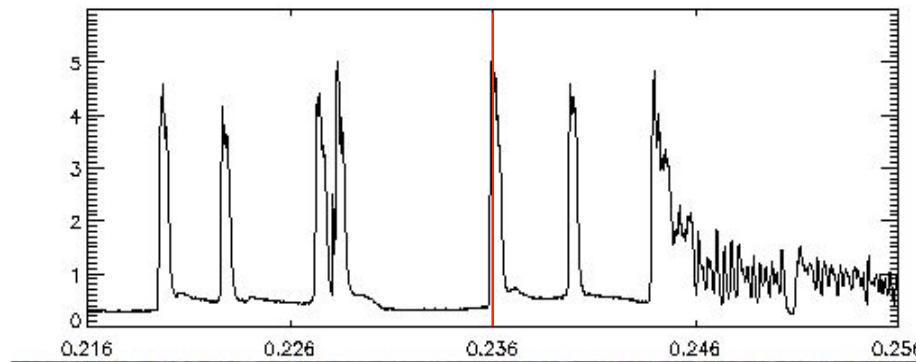
Kink mode:

- Ideal MHD kink mode deforms surface driven by parallel current
- requires a rational q surface just outside plasma
- Magnetic topology remains the same in ideal MHD
- Peeling modes are localised external kink modes driven by the J_{edge}

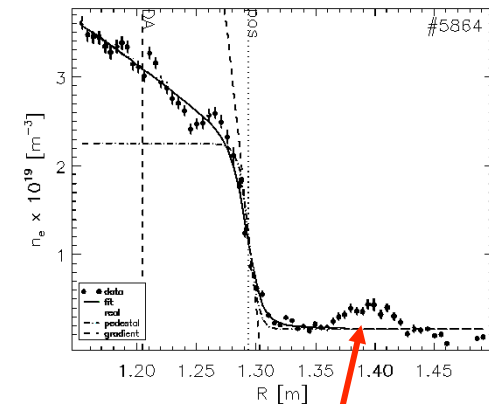
MAST and NSTX Tokamak shows Type I ELMs

R. J. Akers et al, Plasma Phys. Control Fusion 45, A175 (2003)

$D\alpha$



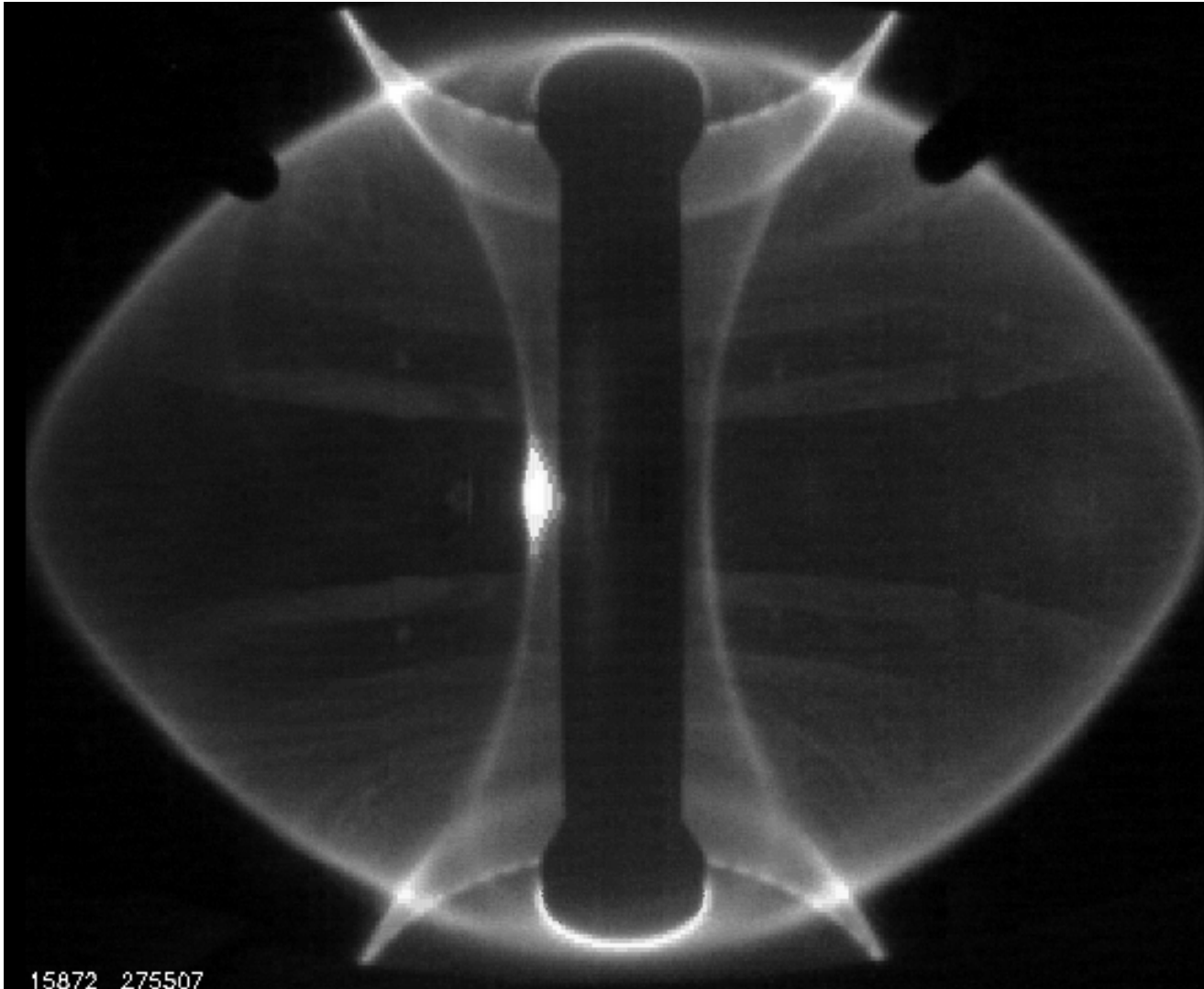
Thompson Scattering



Ballooning Filament

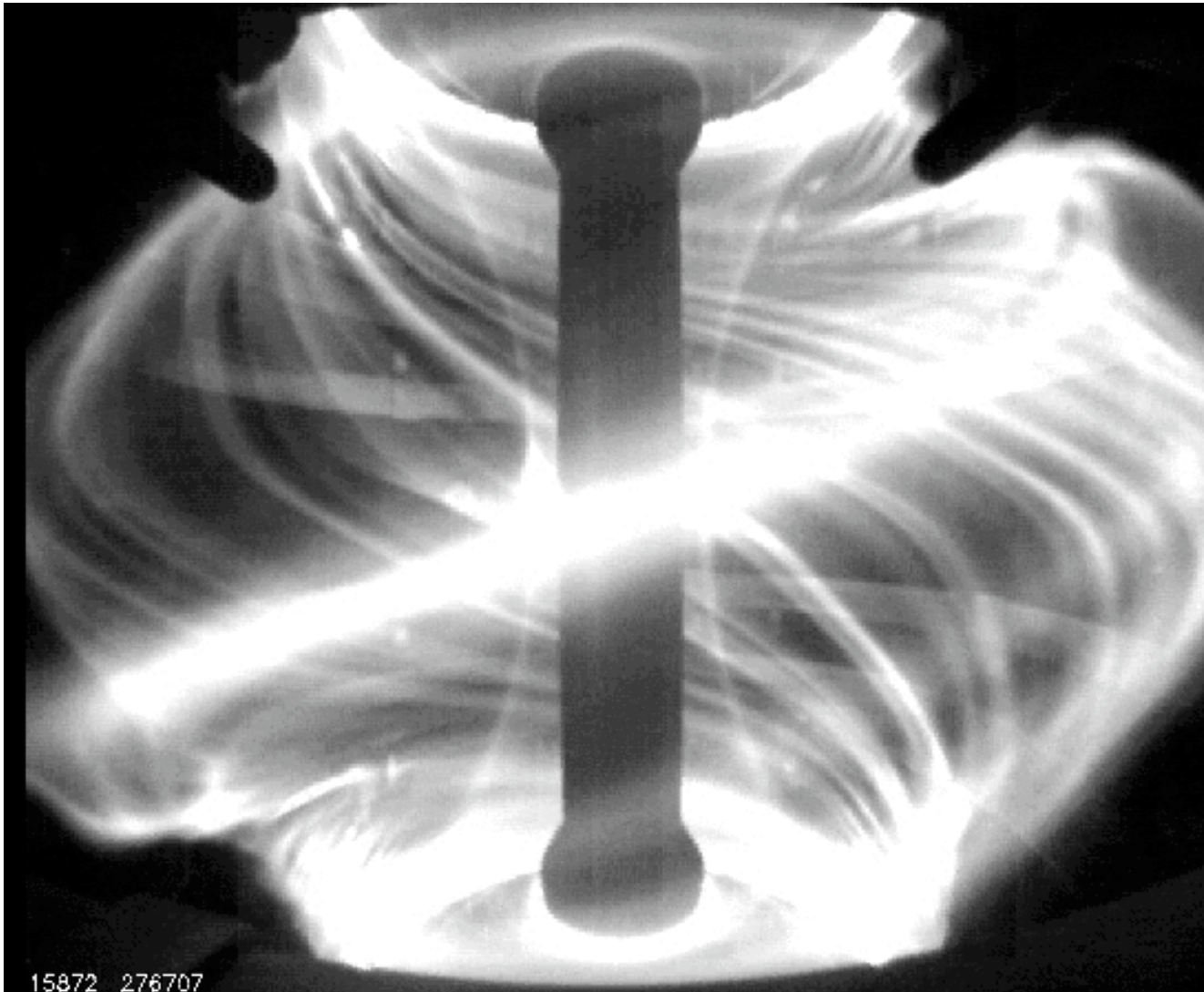
Localized filamentary structure along the field line, appears to be attached to the core for at least $50 \mu\text{s}$. They appears to behave individually in their radial propagation.

Type I ELMs Activity



A. Sykes, ICPP, Fukuoka Sept 2008

Type I ELMs Activity



A. Sykes, ICPP, Fukuoka Sept 2008

Experimental Observations

These typical ELMs have the following characteristics features

- Middle ($n=5\sim 10$) precursor and coexistence of a low- n kink (Type-I)
- Localized filamentary structure along the field line
- Occurrence during the H-mode of operation
- Occurrence near ballooning stability limit
- Convective loss of plasma
- ELM rise time $\sim 100\mu\text{sec}$

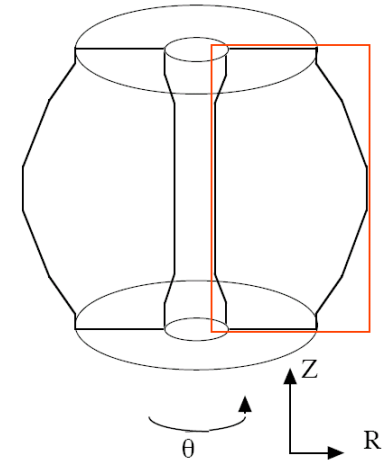
Simulation model

Resistive MHD Model Equations

$$\frac{\partial \rho}{\partial t} = -\nabla \cdot (\rho \mathbf{v})$$

$$\frac{\partial}{\partial t} (\rho \mathbf{v}) = -\nabla \cdot (\rho \mathbf{v} \mathbf{v}) - \nabla p + \mathbf{j} \times \mathbf{B} + \mu (\nabla^2 \mathbf{v} + \frac{1}{3} \nabla (\nabla \cdot \mathbf{v}))$$

- Full toroidal 3D geometry
- 4th-order finite difference
- 4th-order RK method



$$\frac{\partial p}{\partial t} = -\nabla \cdot (p \mathbf{v}) - (\gamma - 1)(p \nabla \cdot \mathbf{v} + \eta \mathbf{j}^2 + \Phi)$$

Convection term + heating terms(adiabatic comp. + ohmic heating + viscous heating)

$$\frac{\partial \mathbf{B}}{\partial t} = -\nabla \times \mathbf{E} \quad \text{(Equation of induction)}$$

$$\mathbf{E} = -\mathbf{v} \times \mathbf{B} + \eta \mathbf{j}; \quad \mathbf{j} = \nabla \times \mathbf{B}$$

(Viscous heating) (rate of strain tensor)

$$\Phi = 2\mu \left(e_{ij} e_{ij} - \frac{1}{3} (\nabla \cdot \mathbf{v})^2 \right); \quad e_{ij} = \frac{1}{2} \left(\frac{\partial v_i}{\partial x_j} + \frac{\partial v_j}{\partial x_i} \right)$$

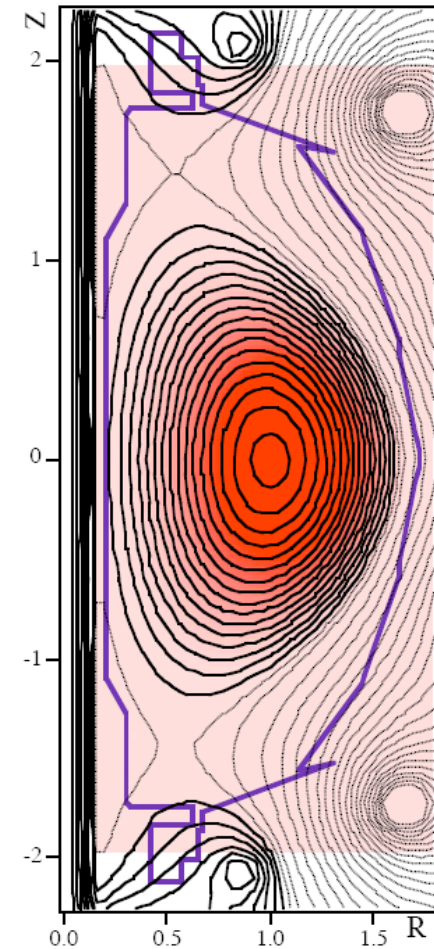
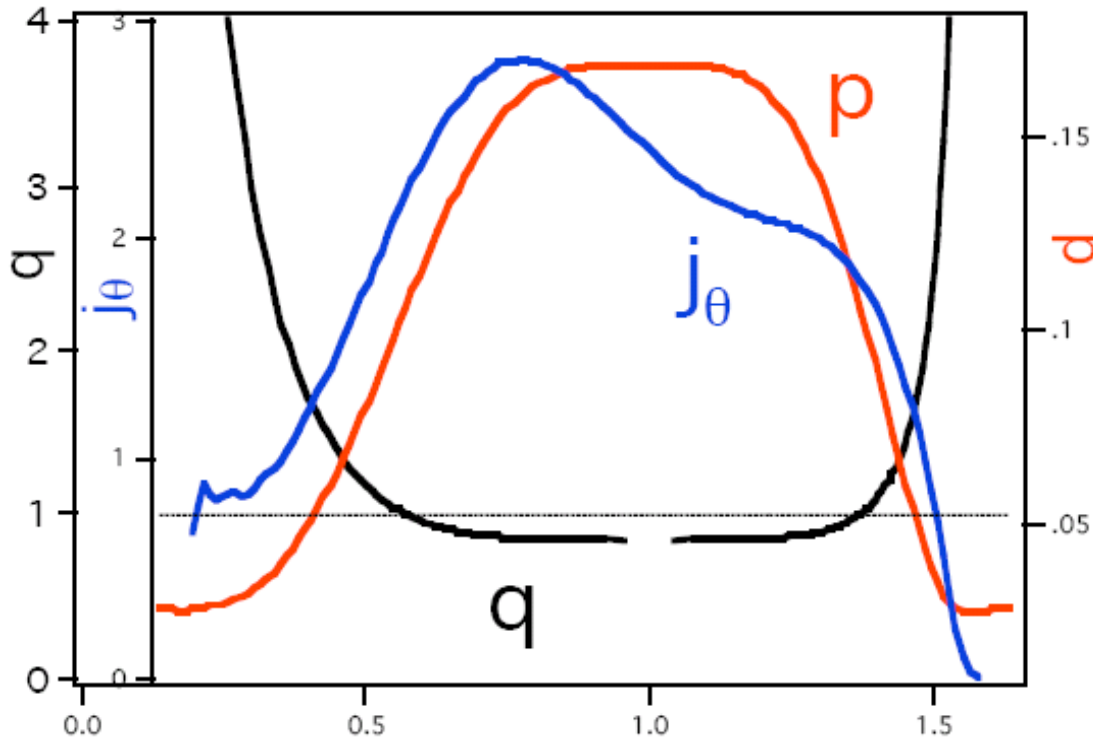
Independent variables

- mass density ρ
- fluid velocity \mathbf{v}
- magnetic field int. \mathbf{B}
- plasma pressure p
- η and μ are unif. const
- $\gamma \sim 5/3$

local energy conservation \rightarrow the plasma heat, kinetic, and magnetic field energies

Initial Equilibrium

EFIT reconstruction data of NSTX by courtesy of Dr. Sabbagh, Dr. Paoletti, and Dr. Kaye



NSTX Shot number #103701

Time 238 msec

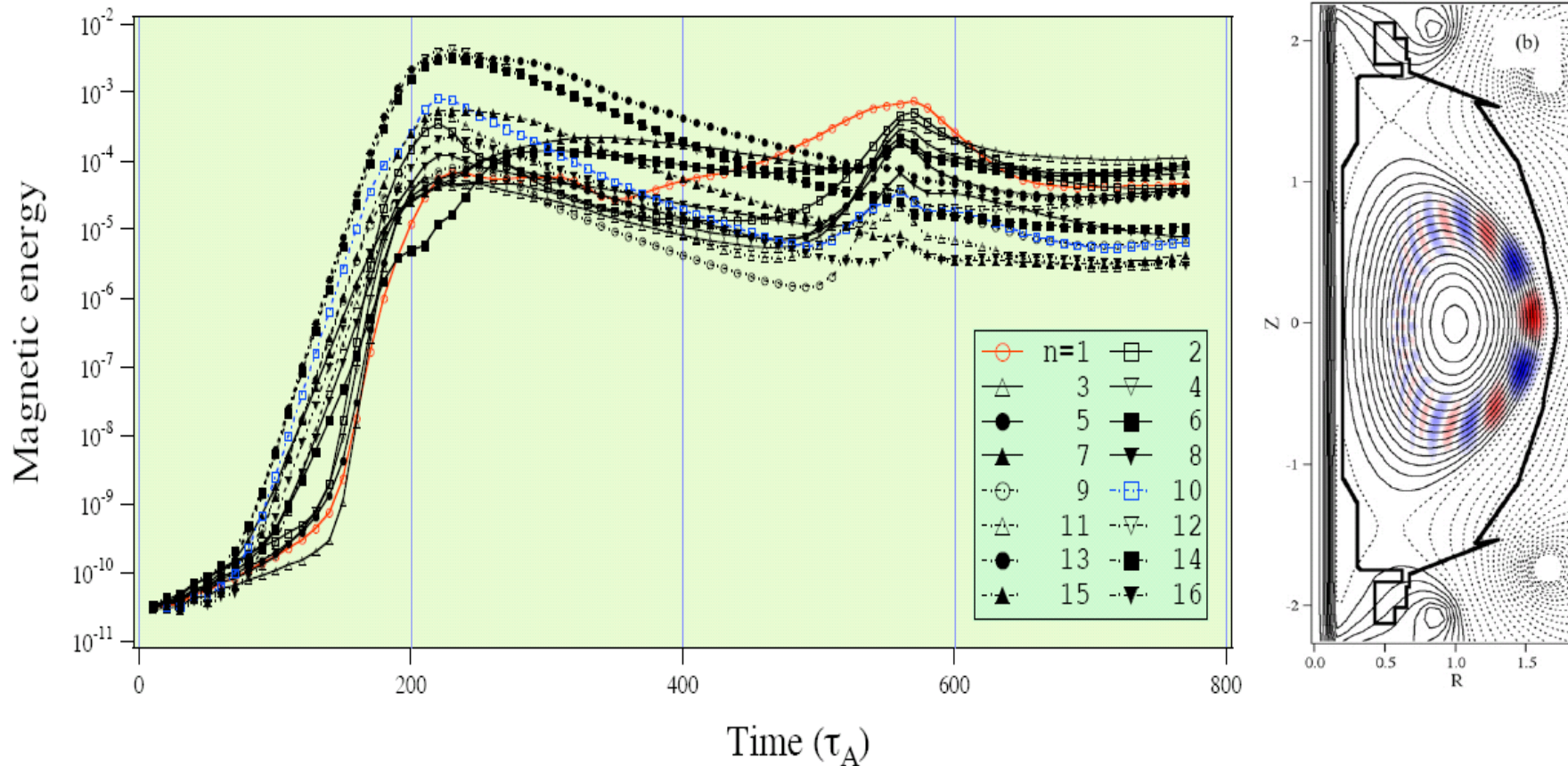
Aspect Ratio 1.4

Central q 0.89

Central beta 28 %

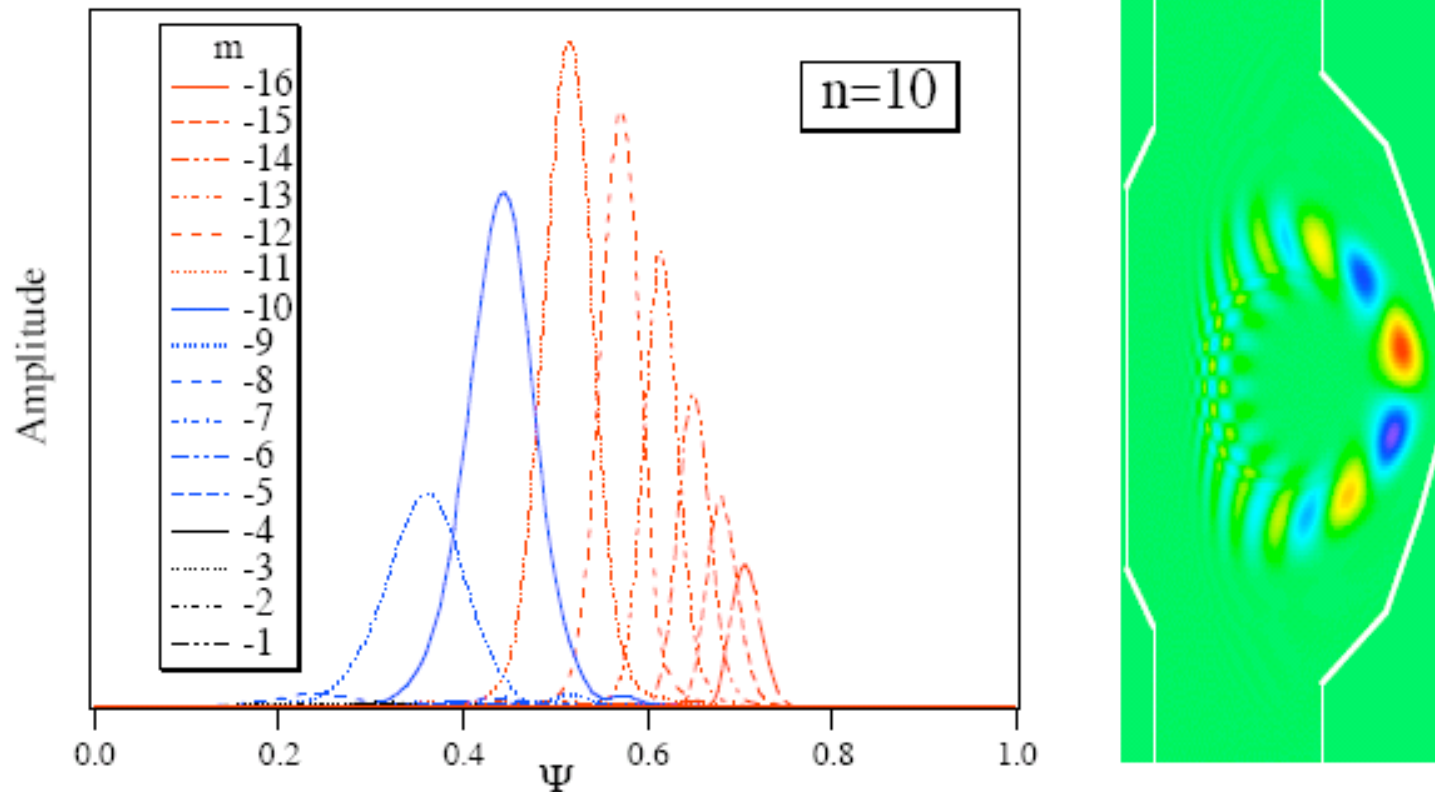
Poloidal flux, pressure,
and conductor boundary

Time development of Energy



- It shows a two-step relaxation process induced by the intermediate- n resistive ballooning mode followed by the $m/n = 1/1$ internal kink mode.
- At $t = 360\tau_A$, only the $n = 1$ mode begins to grow again and ends in internal kink relaxation

Linear Mode Structure

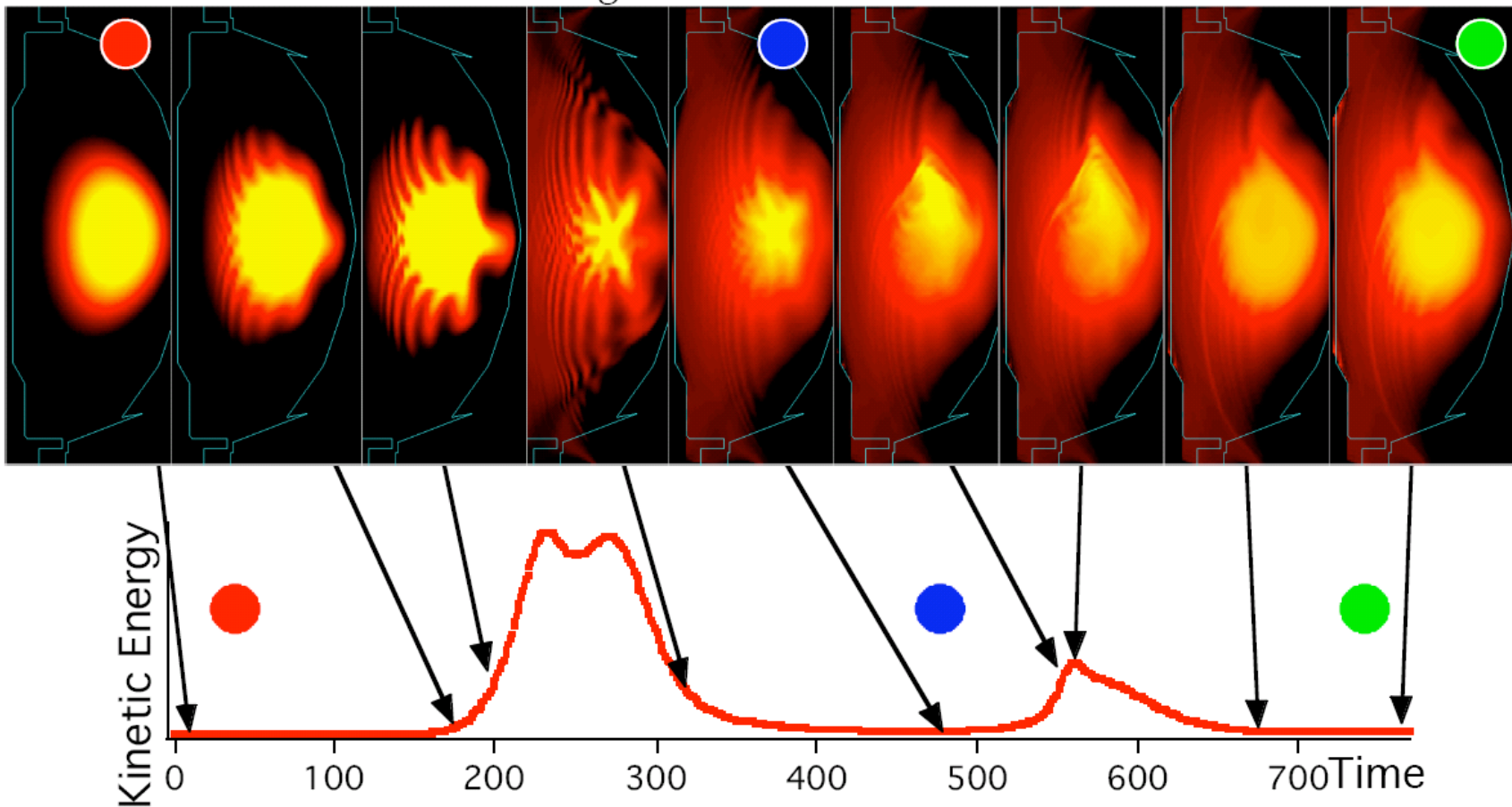


- (a) shows the wide envelop with several poloidal components, superposition of them causes helically expansive deformation.
- (b) The perturbation in the plasma pressure are plotted as contours. It shows that these modes are poloidaly localized and resonant to the relevant rational surface in the bad curvature.

Poloidal Structure of Pressure

Resistive Ballooning

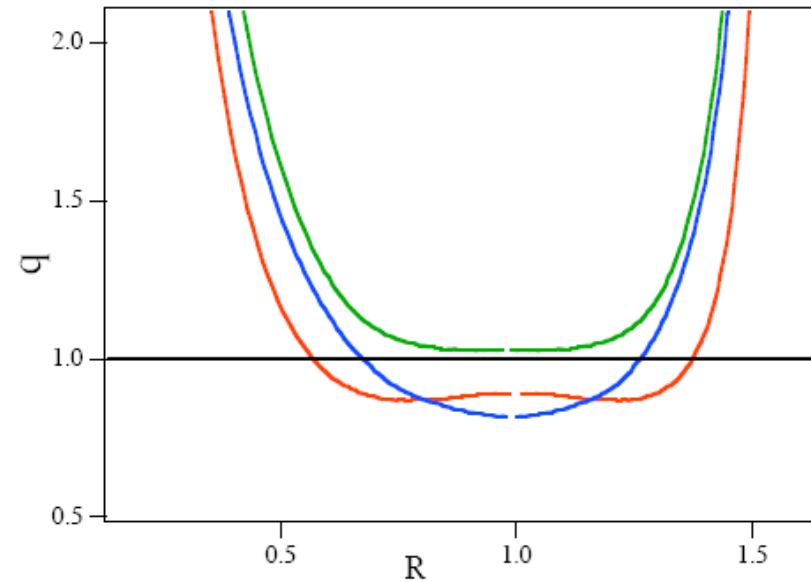
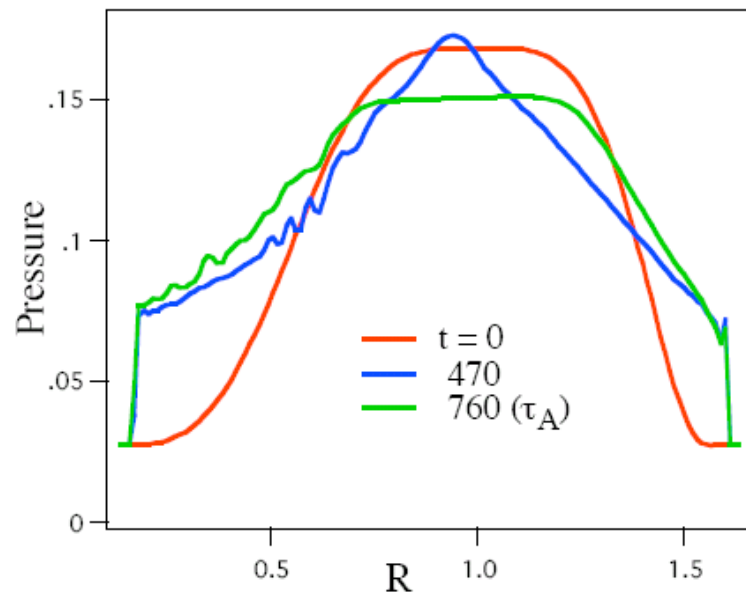
n=1 internal kink



two-step relaxation

1st- intermediate-n ballooning modes, 2nd- n=1 kink mode

Change in Radial Profile

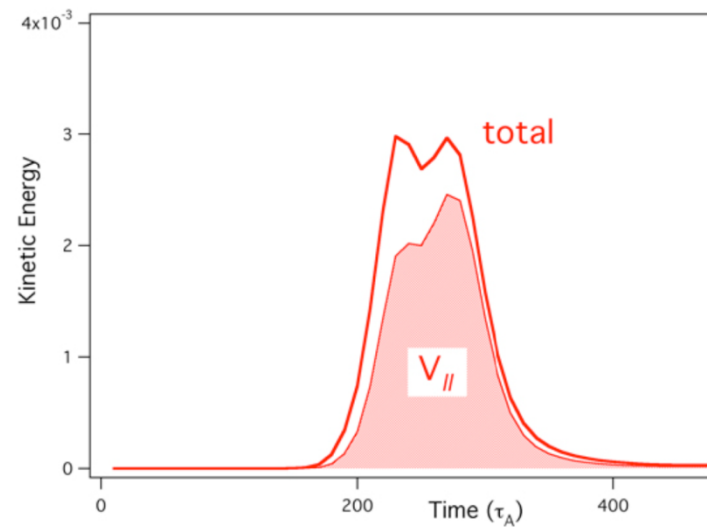
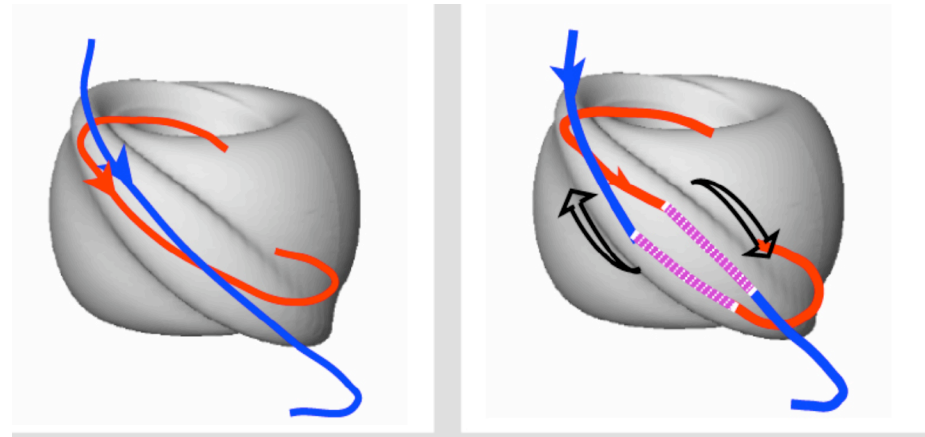


The profile change into a peaked one destabilizes another instability for the 2nd relaxation stage.

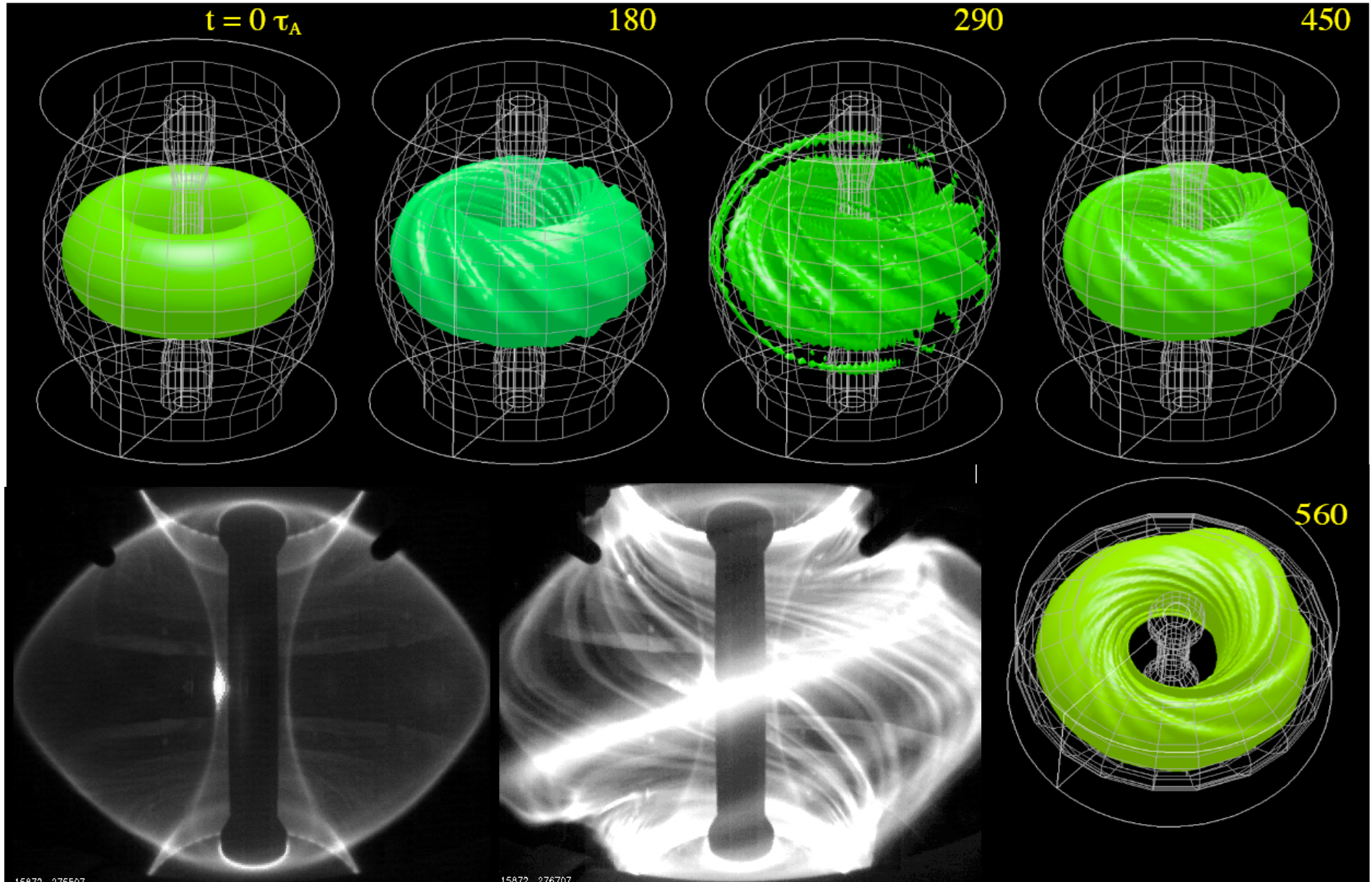
The system finally recovers a broader profile at the core region due to the Kadomchev-type sawtooth crash.

Enhanced plasma loss mechanism through reconnection

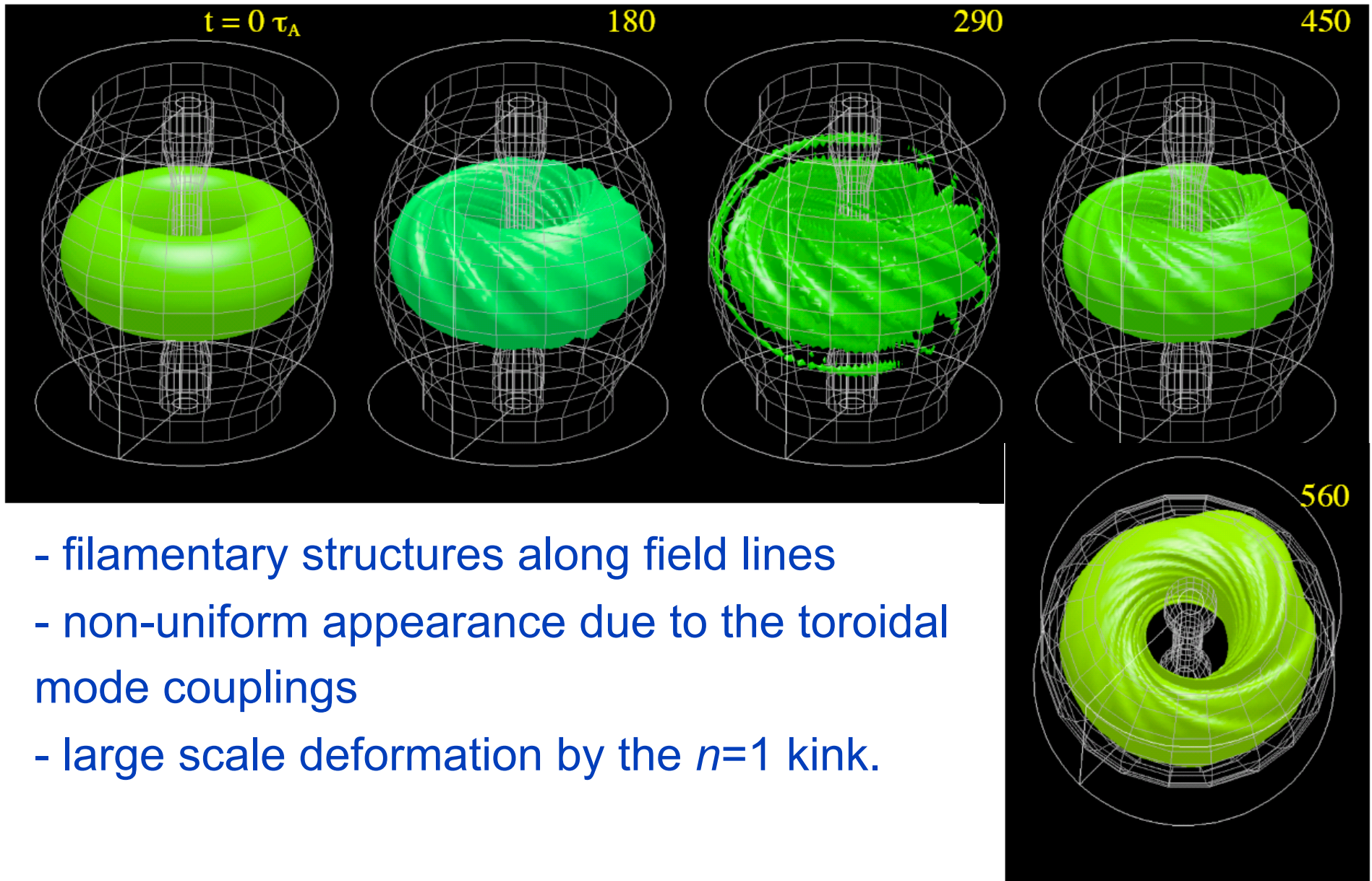
- Perpendicular flows due to the ballooning eruption induces a forced reconnection between the internal and external field.
- Large pressure imbalance formed along the reconnected field lines causes a parallel outward



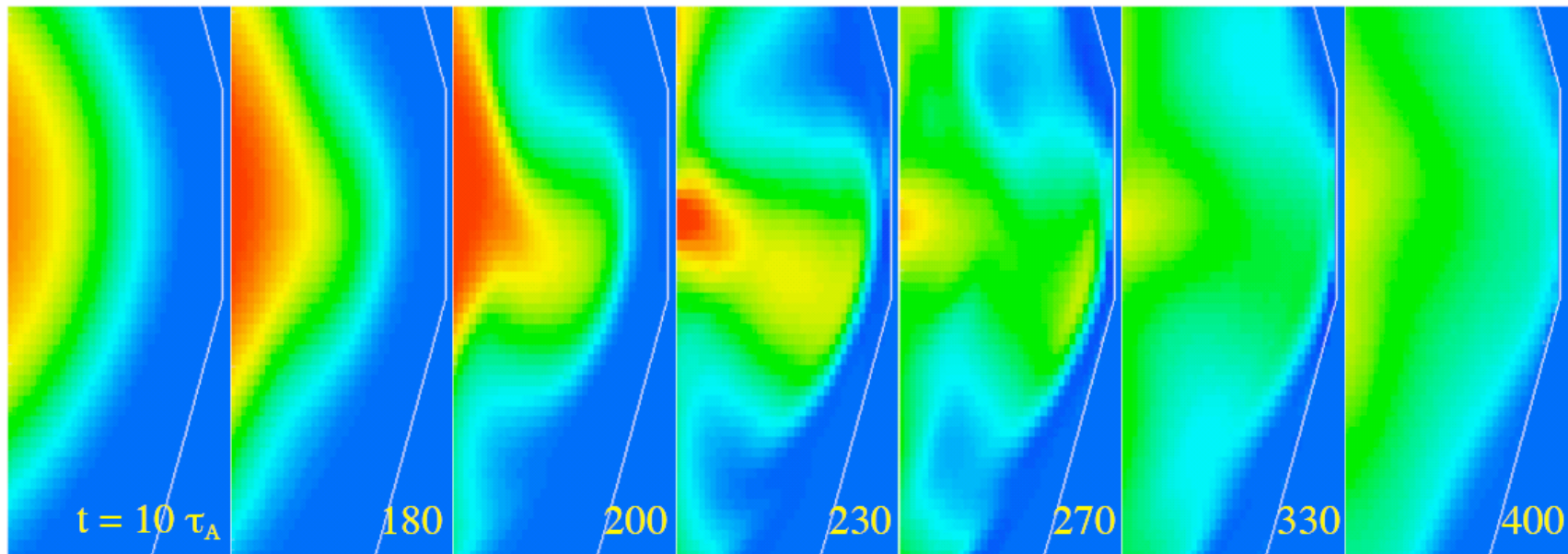
3D Structure



3D Structure

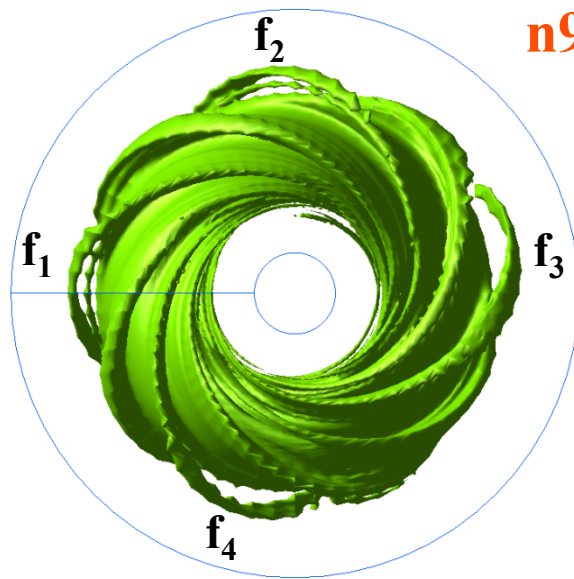


Ejection of plasmoid

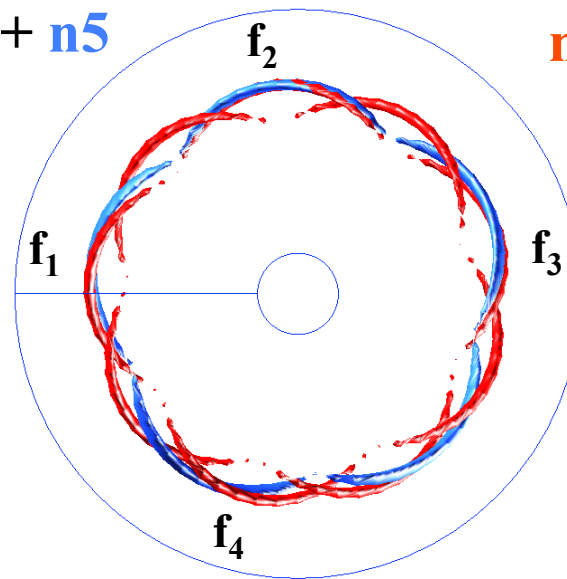


- fragment of plasma is separated from the core on a ridge of the filaments

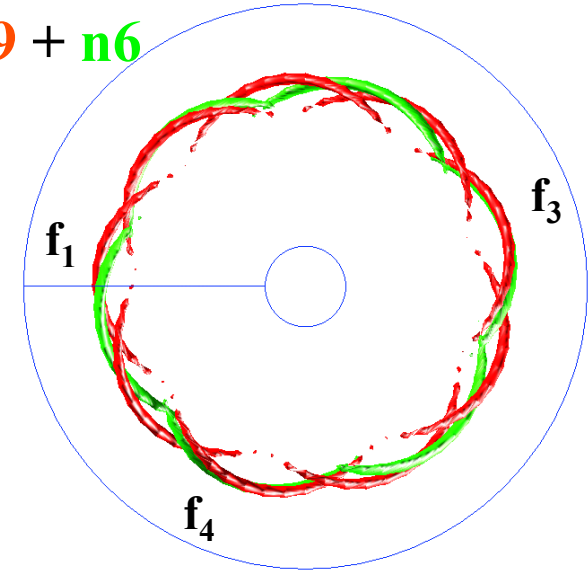
Toroidal Coupling



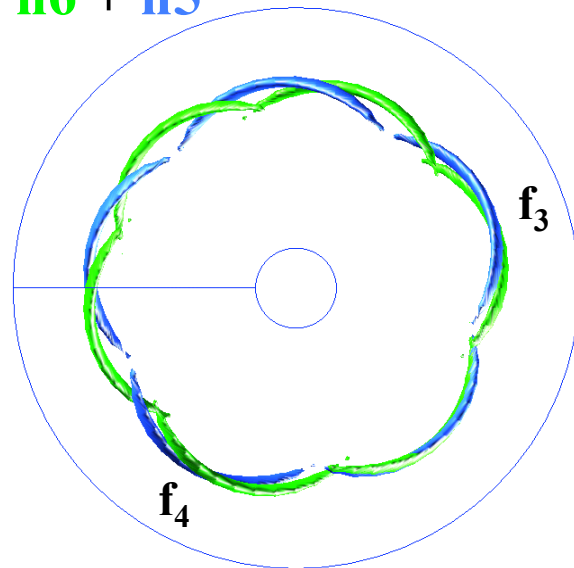
n9 + n5



n9 + n6



n6 + n5



n9 ($m/n=11/9=1.22$), **n6** ($m/n=7/6=1.16$),

n5 ($m/n=6/5=1.20$)

It shows that rational surface of n9 and n5 are closer to one another which enhance the probability of toroidal coupling between n9 and n5.

Comparison With Experiments

1) Unique structures

(filaments along field lines, separation of plasmoid, $n=1$ kink)

2) Triggering by the ballooning mode

3) ELM rise time scale ($\sim 100 \mu\text{sec}$)

4) Convective loss of plasma from the edge

5) Succession of the intermediate- n precursor and $n=1$ fluctuation

6) Inward propagation of perturbations

“Good agreement with the Type-I ELM properties”

The drift model (the ion diamagnetic effect)

Standard MHD model neglects the finite Larmor radius (FLR). Which introduce global rotation of perturbation both toroidally and poloidally, which makes the model more realistic to the experimental phenomena.

$$\frac{\partial \rho}{\partial t} = -\nabla \cdot \mathbf{v}$$

$$\rho \frac{\partial \mathbf{v}_M}{\partial t} = -\rho \mathbf{v} \cdot \nabla \mathbf{v}_E - \rho \mathbf{v}_M \cdot \nabla (\mathbf{b} V_{\parallel}) - \nabla p + \mathbf{j} \times \mathbf{B}$$

$$\frac{\partial \mathbf{B}}{\partial t} = -\nabla \times \mathbf{E}$$

$$\mathbf{v} = \mathbf{v}_M + \mathbf{v}_p$$

MHD velocity

$$\frac{\partial p}{\partial t} = -\nabla \cdot (p \mathbf{v}_M) - (\gamma - 1) p \nabla \cdot \mathbf{v}_M + Q$$

$$\mathbf{v}_p = \frac{m}{2e} \frac{\mathbf{B} \times \nabla p}{\rho B^2}$$

diamagnetic drift velocity

$$\mathbf{j} = \nabla \times \mathbf{B}$$

$$\mathbf{E} = -\mathbf{v} \times \mathbf{B} + \eta \mathbf{j} + \frac{m}{2e} \frac{\nabla p}{\rho} - \frac{m}{e} \frac{\mathbf{j} \times \mathbf{B}}{\rho}$$

Hazeltine and Meiss Model (Plasma conf. 2003), and Chang and Callen Model (POF B4(7) 1992).

$$- \mathbf{v}_p^{sim} = \alpha \cdot \mathbf{v}_p^{real}$$

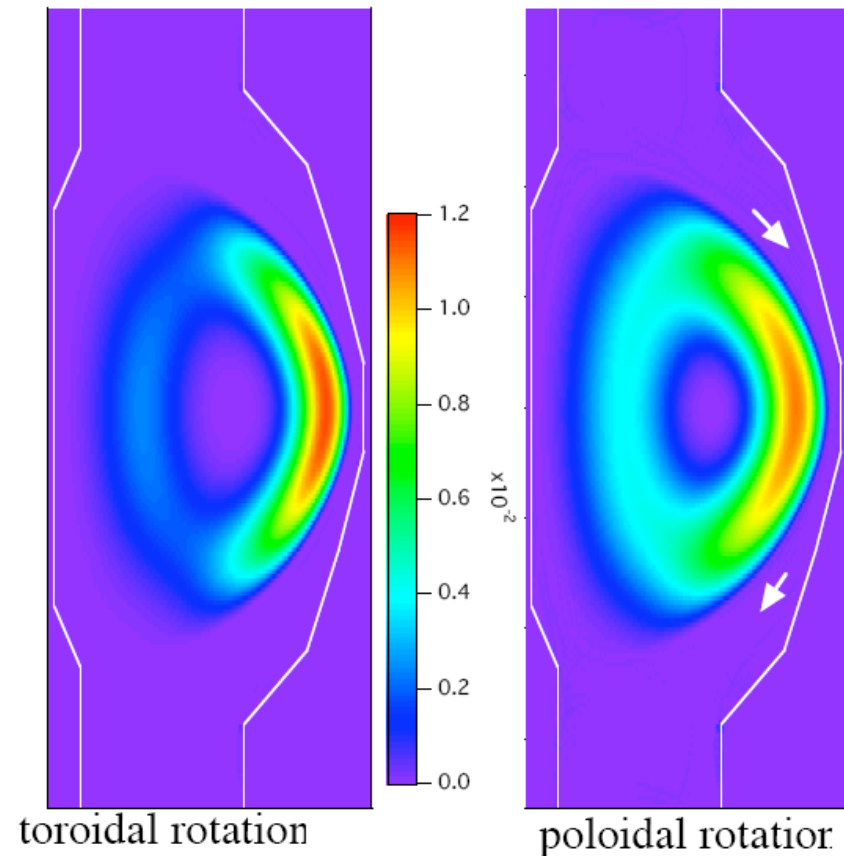
(α : control parameter)

- ignore the electron dynamics - uniform density

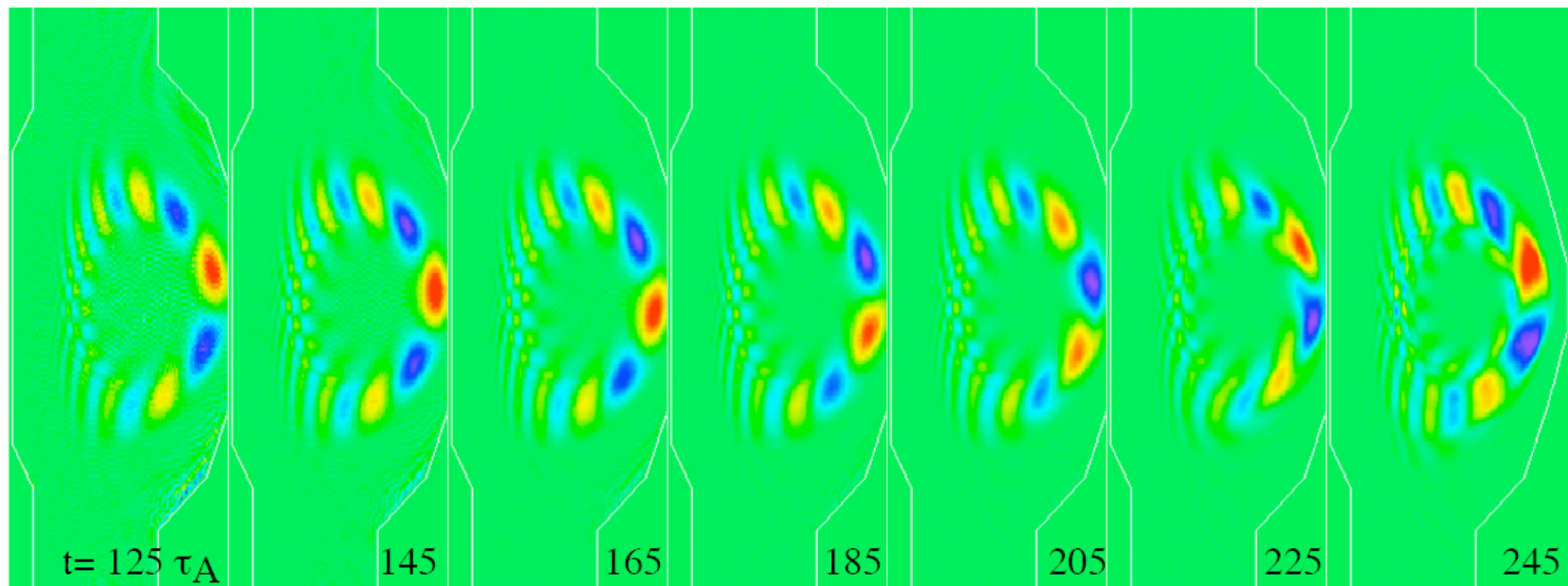
The diamagnetic flows driven by the pressure gradient, are known to have a stabilizing influence on ideal MHD modes.

Rotation of the Modes Structure

- The advection term added in the equation of motion introduces a global rotation of perturbation both in toroidal as well as poloidal directions.
- A narrow flow shear band exist in edge region.

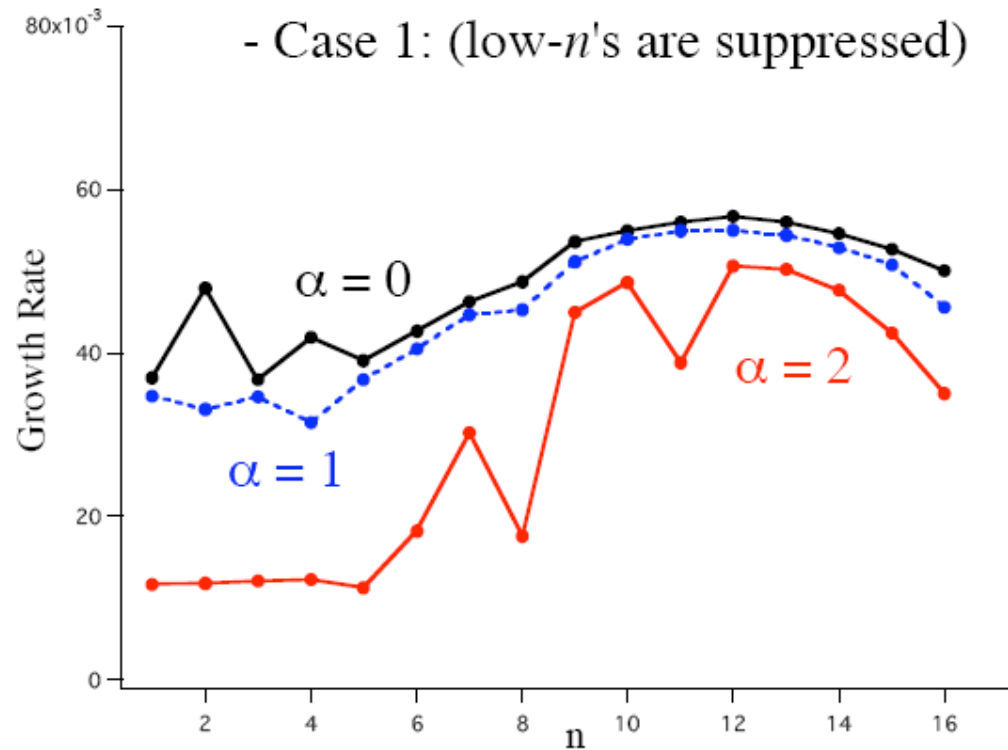


Rotation of the Modes Structure



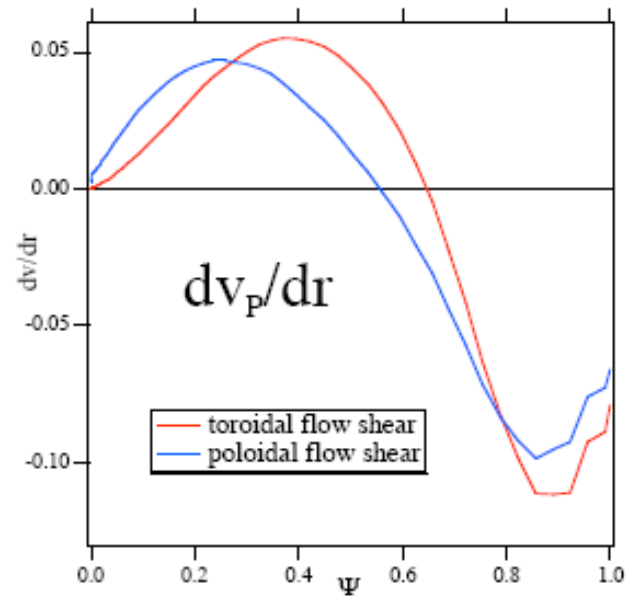
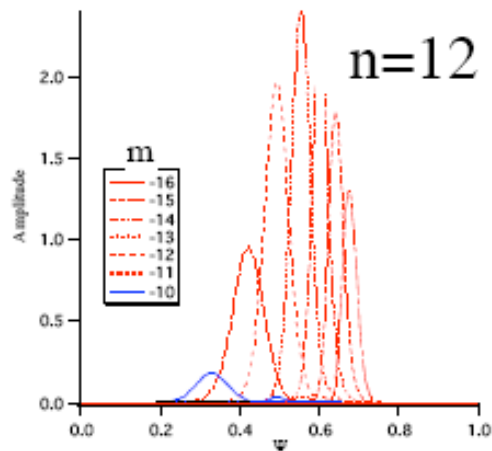
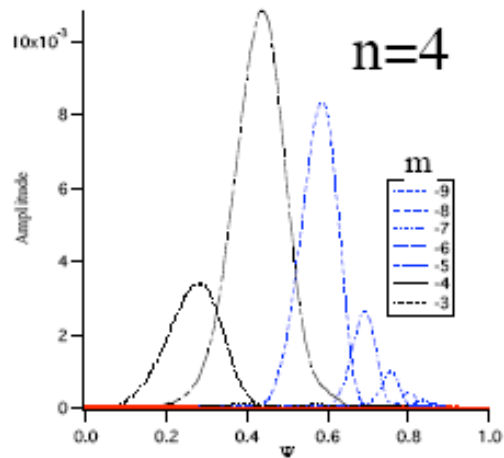
- The advection term added in the equation of motion introduces a global rotation of perturbation both in toroidal as well as poloidal directions.

Growth rate of linear instabilities



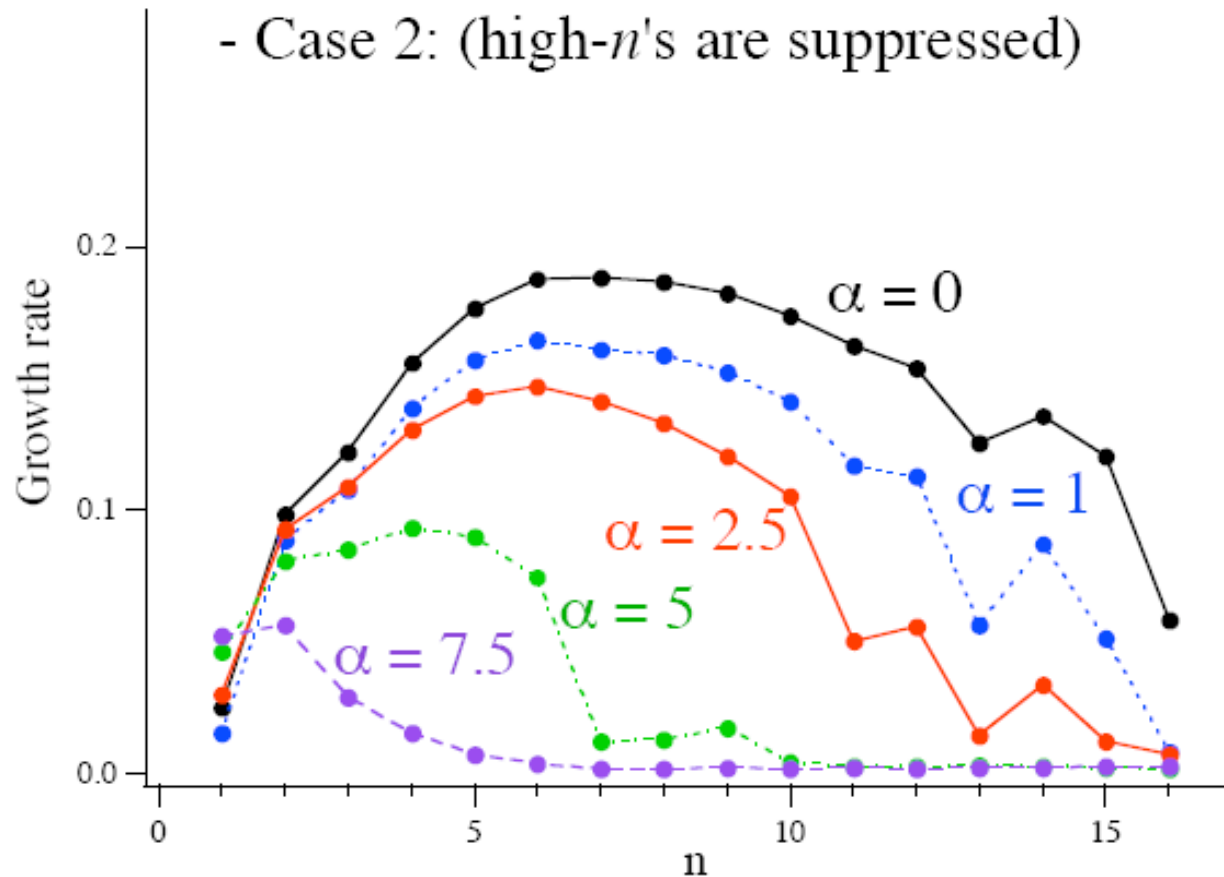
- Stabilizing effect would depend on the relation between the mode and diamagnetic flow structure

Structure of diamagnetic flow



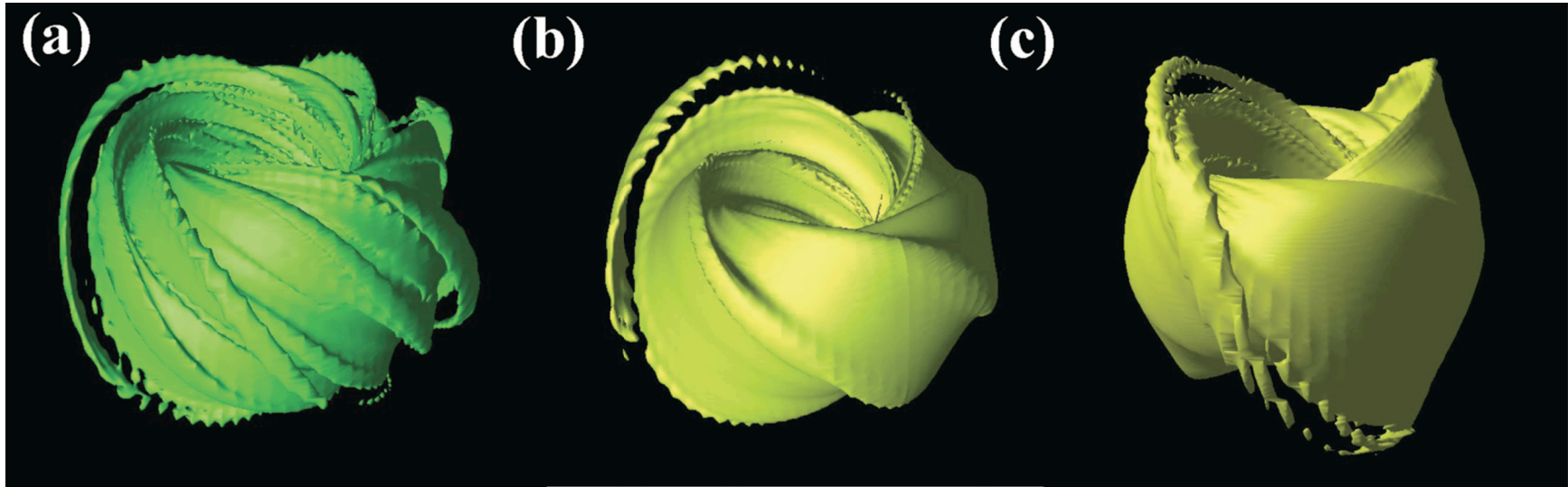
Suppression of the linear instability is much affected by the location of the diamagnetic flow shear, and therefore is sensitive to the profile.

Growth rate of linear instabilities



Suppression of the linear instability is much affected by the location of the diamagnetic flow shear, and therefore is sensitive to the profile. 28

Comparison of Filaments



- The filaments are formed universally because of the toroidal mode coupling, despite the dominant linear mode number changes.
- There is no significant effect on the linear instability for the realistic parameter range.

Concluding remarks

- Numerical simulation based on MHD model have been executed for the purpose of revealing the nonlinear dynamics of the ballooning mode (pressure driven) and Peeling mode (current driven) in toroidal plasma.
- The simulation results corresponding to the ELM crash phase in Tokamak plasma have reproduced experimental observations.

Concluding remarks

- There is good agreement between the simulation and experiments in forming the filamentary structures, separation of plasmoid from the core, time scale, etc..
- A successional $n=1$ activity are induced spontaneously by the profile change.
- Non-uniformity of the filaments are reproduced by the toroidal mode couplings
- Reconnection between the internal and external fields and related parallel flows enhance the loss of plasma.

Concluding Remarks

- Modification of MHD model by using simplified drift model, has been found to suppress the n components linearly, since the mode growth is suppressed by the sheared rotation flows.
- The filaments are formed universally because of the toroidal mode coupling, despite the dominant linear mode number changes.
- There is no significant effect on the linear instability for the realistic parameter range.

THANKS

Comparison between peeling and ballooning mode

In order to obtain a peeling-unstable equilibrium, we assume

1) large edge current

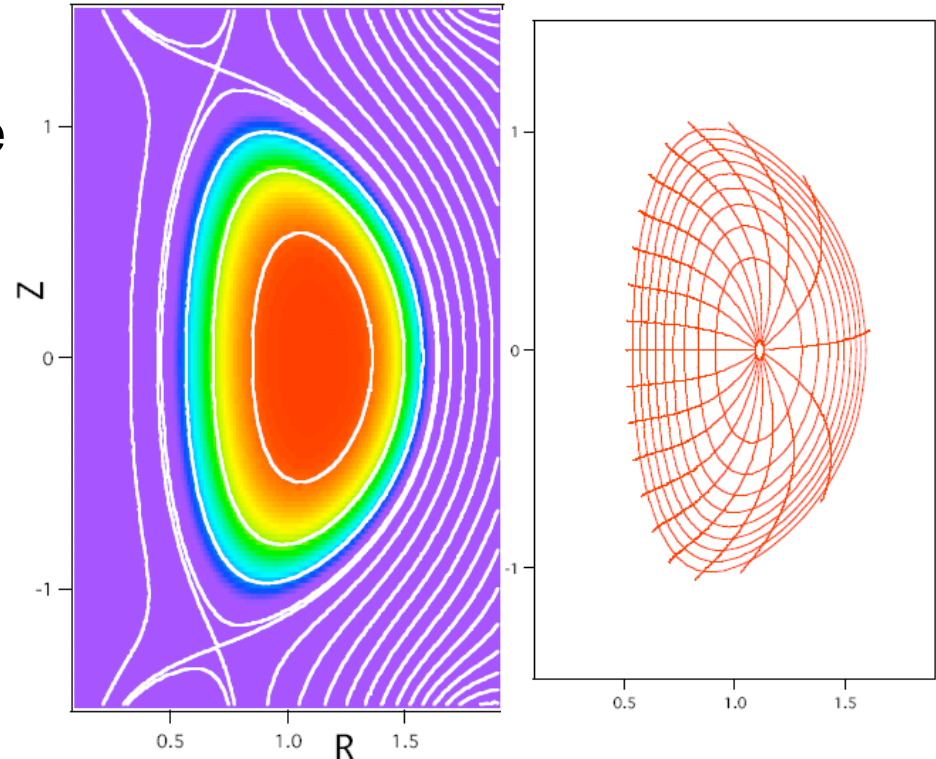
→ to destabilize the current-driven mode by increasing current in the region where the pressure gradient is steep

2) isolation from the wall

→ to disable the wall stabilization for the external modes (i.e. uses double null diverter config and far off conducting boundaries)

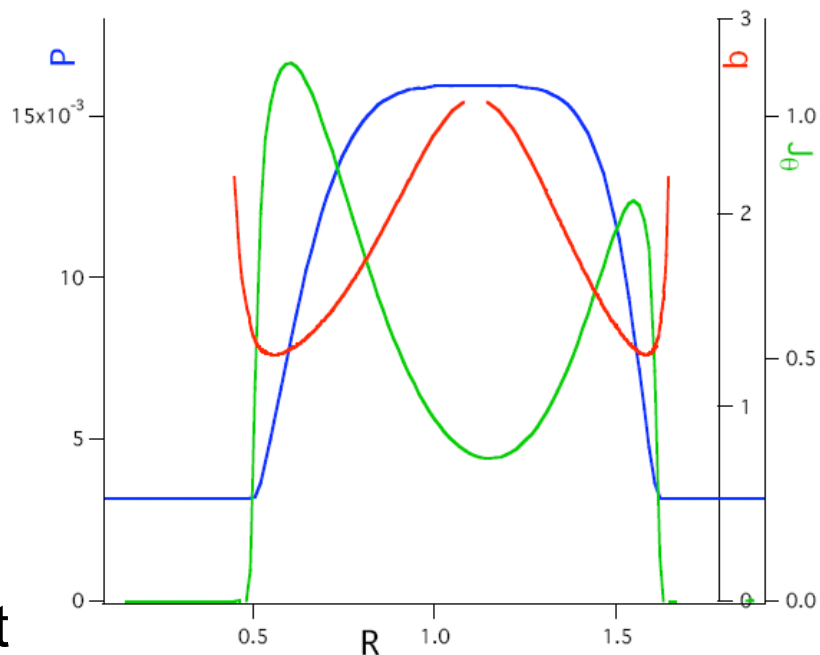
3) larger triangularity

→ to suppress the ballooning mode

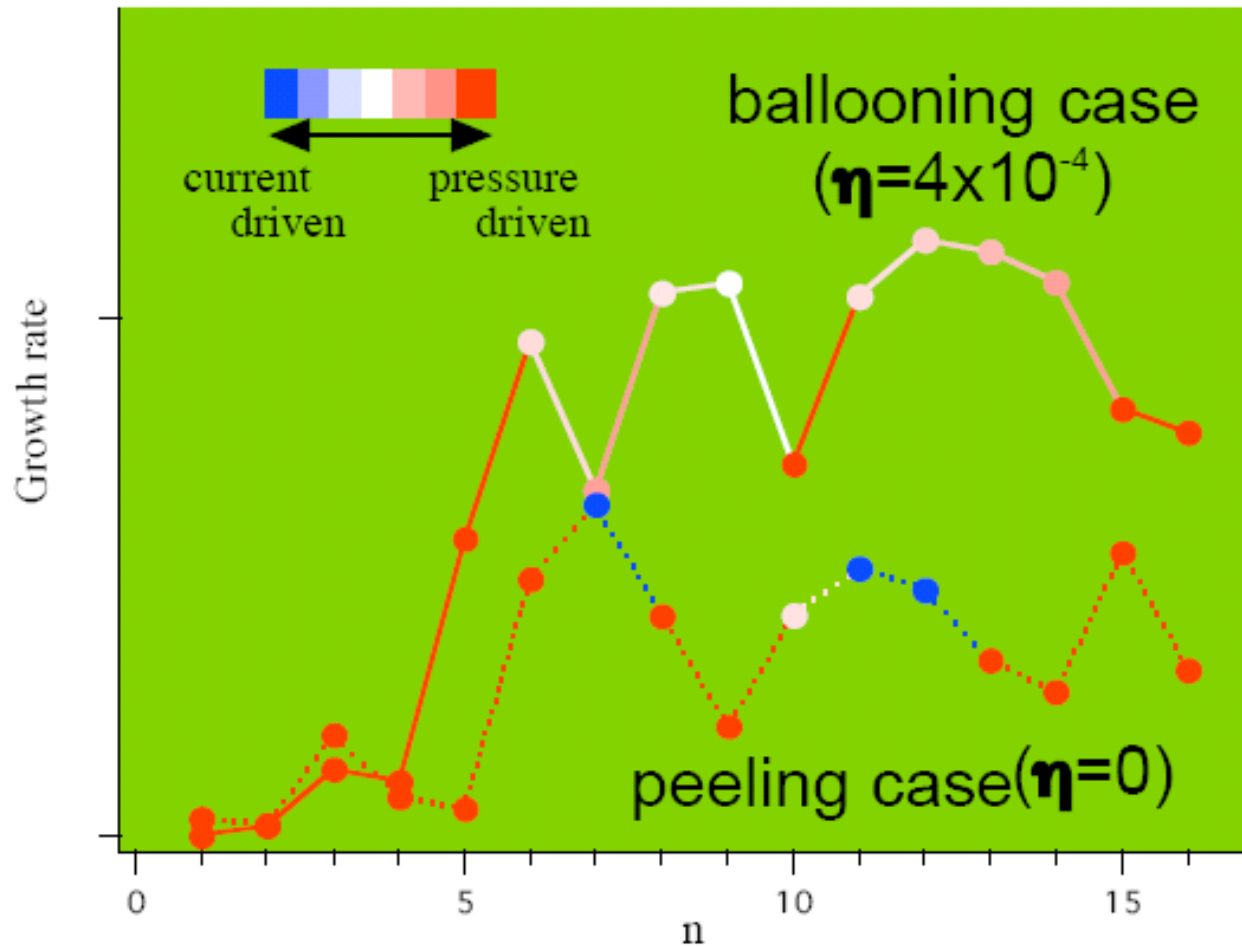


Radial pressure, current, and q profiles

- Solve the Grad-Shafranov equation in a poloidal 2-D rectangular grid
- Calculate the external vacuum field by summing up the current of the external coil and the plasma
- The pressure is broad, the current is highly hollow
- The safety factor profile is strong negative-sheared with $\beta_0=25\%$, $\langle\beta\rangle \sim 5\%$, $A=2.0$, and $q_{\min}=1.27 \leq 9/7$.



Linear instabilities

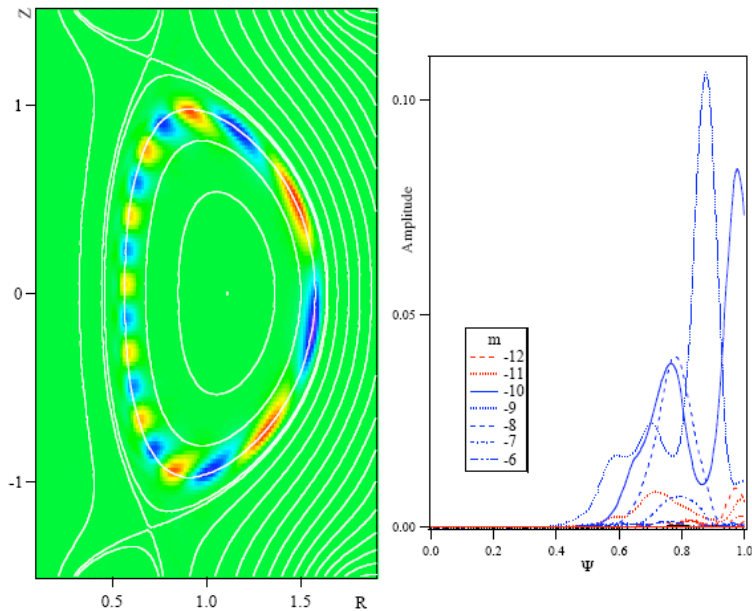


- Ideally unstable to some peeling modes such as $n=7, 11,$ and 12 .
- ballooning unstable for larger η .

Poloidal Mode Structure

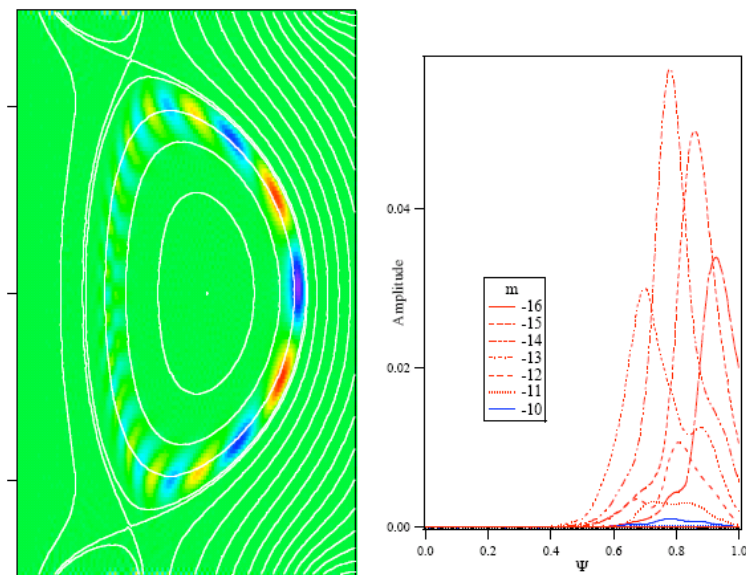
peeling case

($\eta=0, n=7$)



ballooning case

($\eta=4 \times 10^{-4}, n=10$)

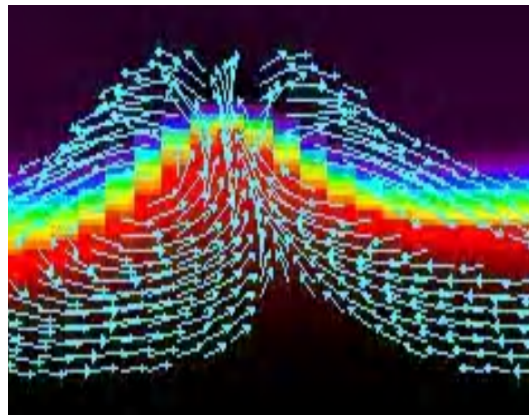


The peeling mode structures are not poloidally localized, they extend towards the edge without any significant poloidal mode couplings.

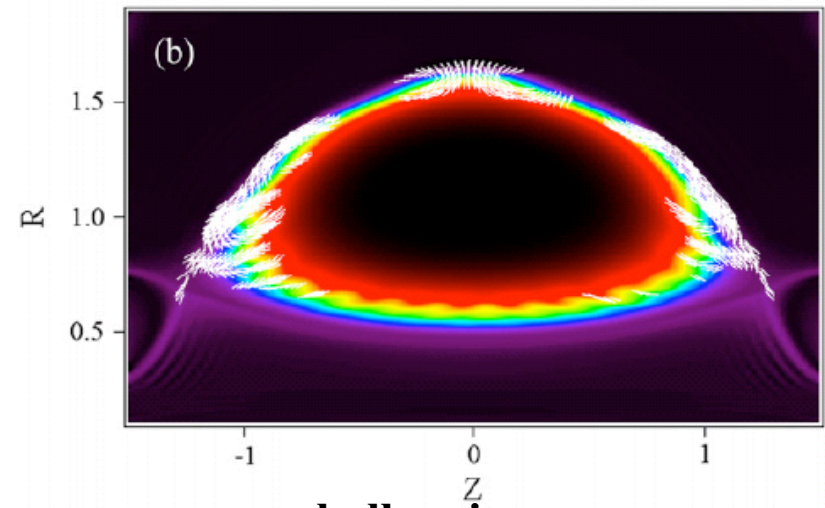
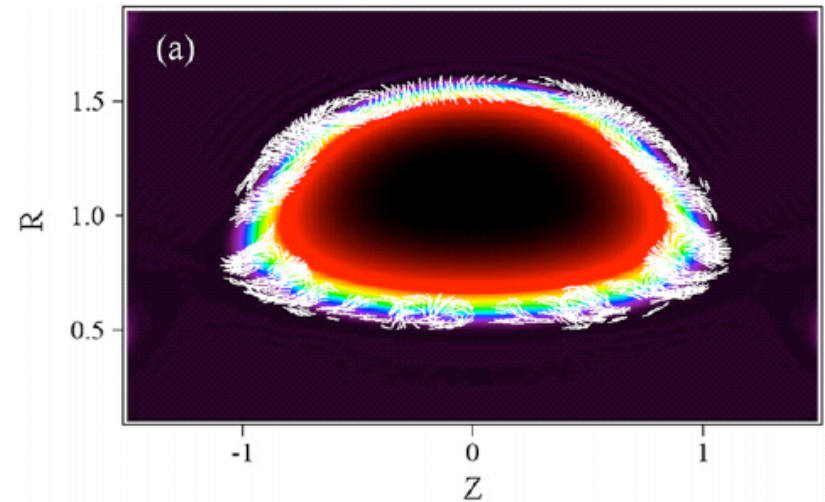
Flow Pattern

The flow pattern shows that the component along the flux surface is significant, in contrast to the ballooning case, where the outward flow is outstanding.

Only the region near surface is perturbed in the peeling case. The high-field side is also perturbed largely.



peeling case



ballooning case

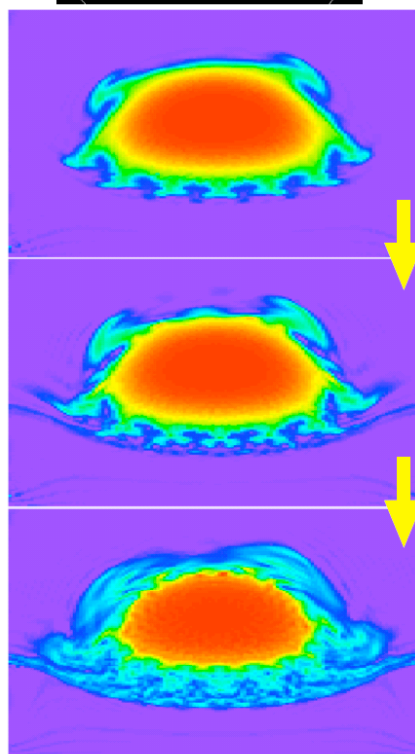
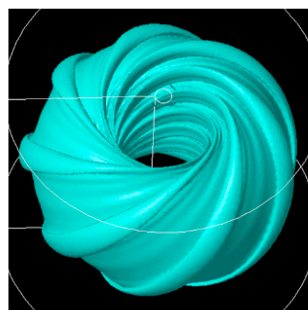
Difference in the nonlinear dynamics

- Filament appears only in the case of the ballooning mode.
- The core region is not so perturbed in the peeling-mode case.
- The toroidal mode coupling should be noted for the ballooning-mode case.

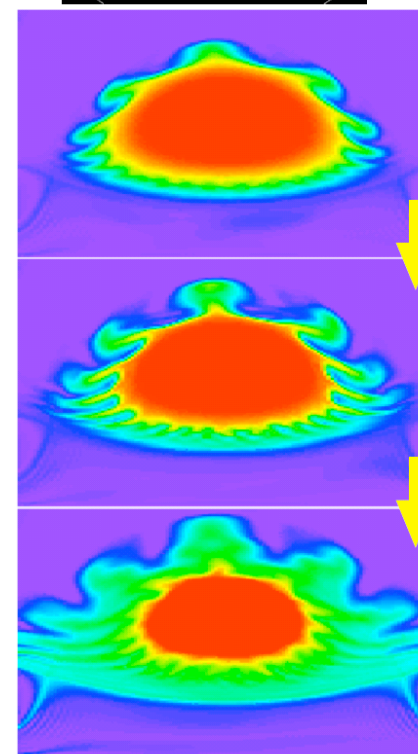
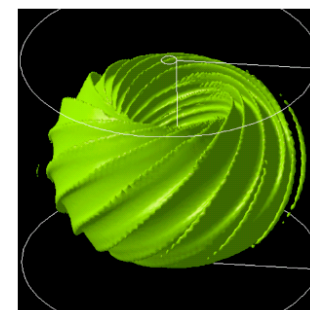
Qualitative difference:

The large ELM activities might be related to the ballooning one.

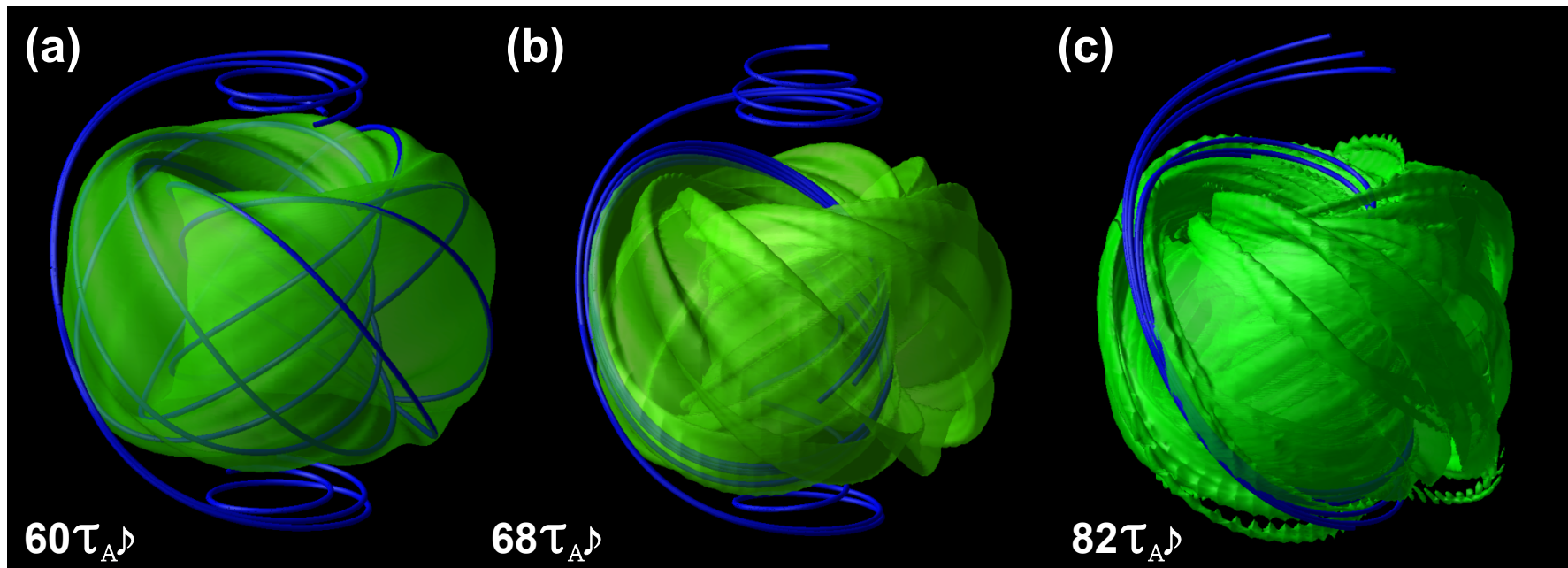
peeling case



ballooning case

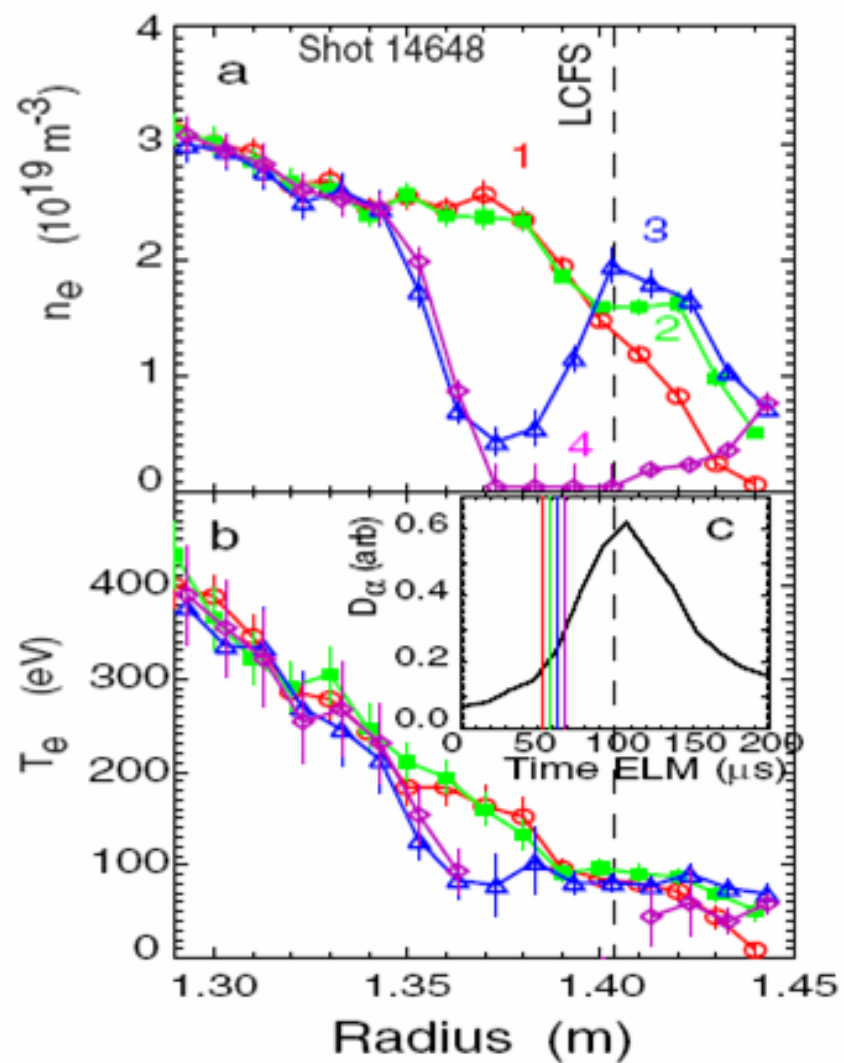
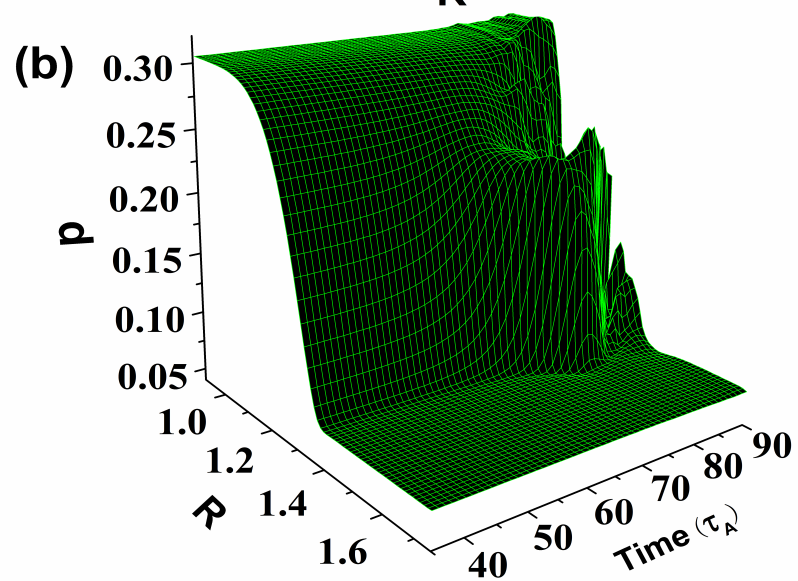
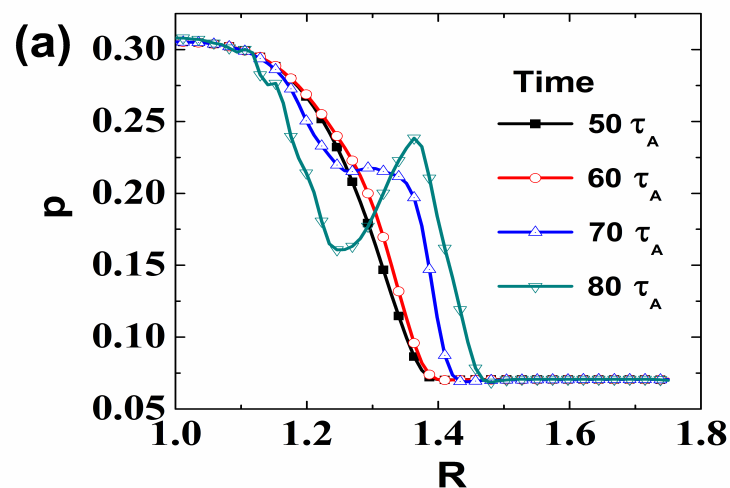


Magnetic Reconnection

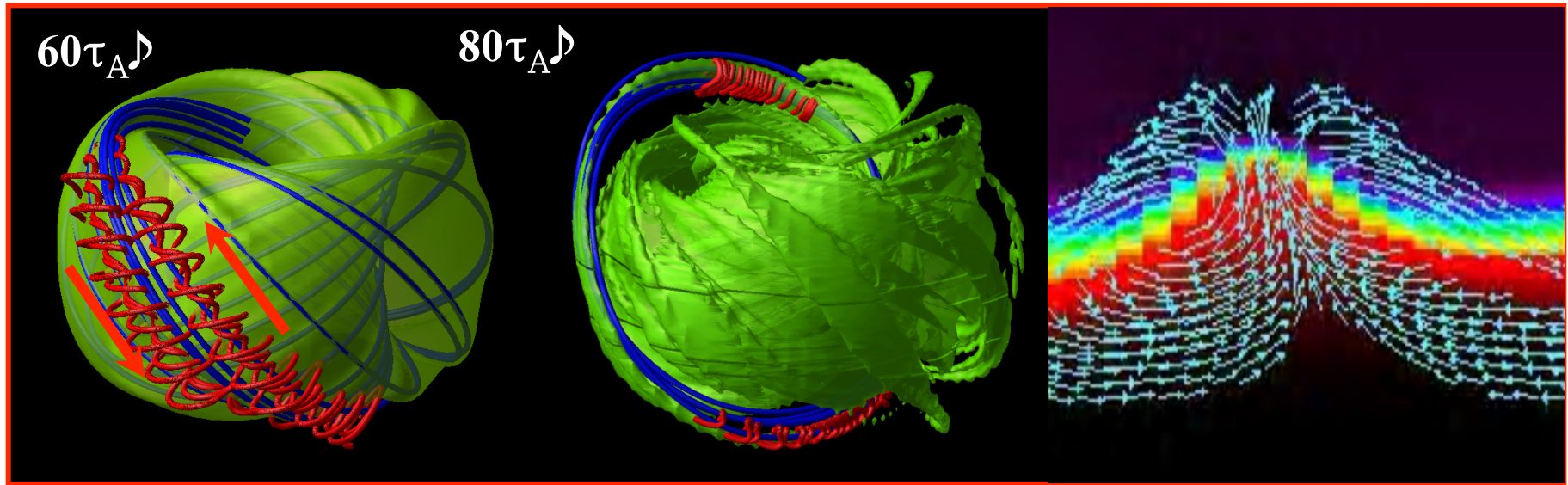


When the balloons is formed at the plasma surface, the magnetic field lines on both side of separatrix are pushed against each other by such perpendicular flow due to spouting out. Under such condition reconnection of the field line can be effectively occurs by driven reconnection mechanism.

Nonlinear Dynamics



Plasma Flow, Magnetic field line and Pressure Iso-surface



- The filamentary structure are formed roughly following the magnetic field lines on the plasma surface. This structure is correspondent with the convection motion of plasma flows, which forms twin vortex pattern.
- Material at the top of the mode's extent is moving horizontally apart in order to allow the plasma in the center of finger to move vertically upward.
- This results in formation of localized bulge of plasma in the form of finger with the steepening of pressure gradient in pedestal region causing the eruption of filaments from edge region.

Normalization

- The magnetic field is normalized by the value of magnetic axis in the initial equilibrium B_o .
- Since pressure same order as energy density, that is, square of magnetic field, hence pressure is automatically normalized by scaling magnetic field, $p_o = (B_o)^2$
- The special scale is normalized by major radius of geometric center of the simulation region.
- The normalization for velocity is given as the Alfvén velocity at the magnetic axis $v_o = B_o / (\rho_o)^{1/2} = B_o$
- The time scale is normalized by the Alfvén transit time at magnetic axis for the length of the major radius of the geometric center.

Two important parameters in MHD stability: q , β

Safety Factor q

- Greater stability higher value of q
- In an equilibrium configuration each magnetic field line has a value of q and follows a helical path around the torus on its own magnetic surface.
- Magnetic surfaces with rational values of q are very important in stability analysis and called resonant surface.

$$q = \frac{\Delta\phi}{2\pi} = \frac{m}{n}$$

Beta Value β

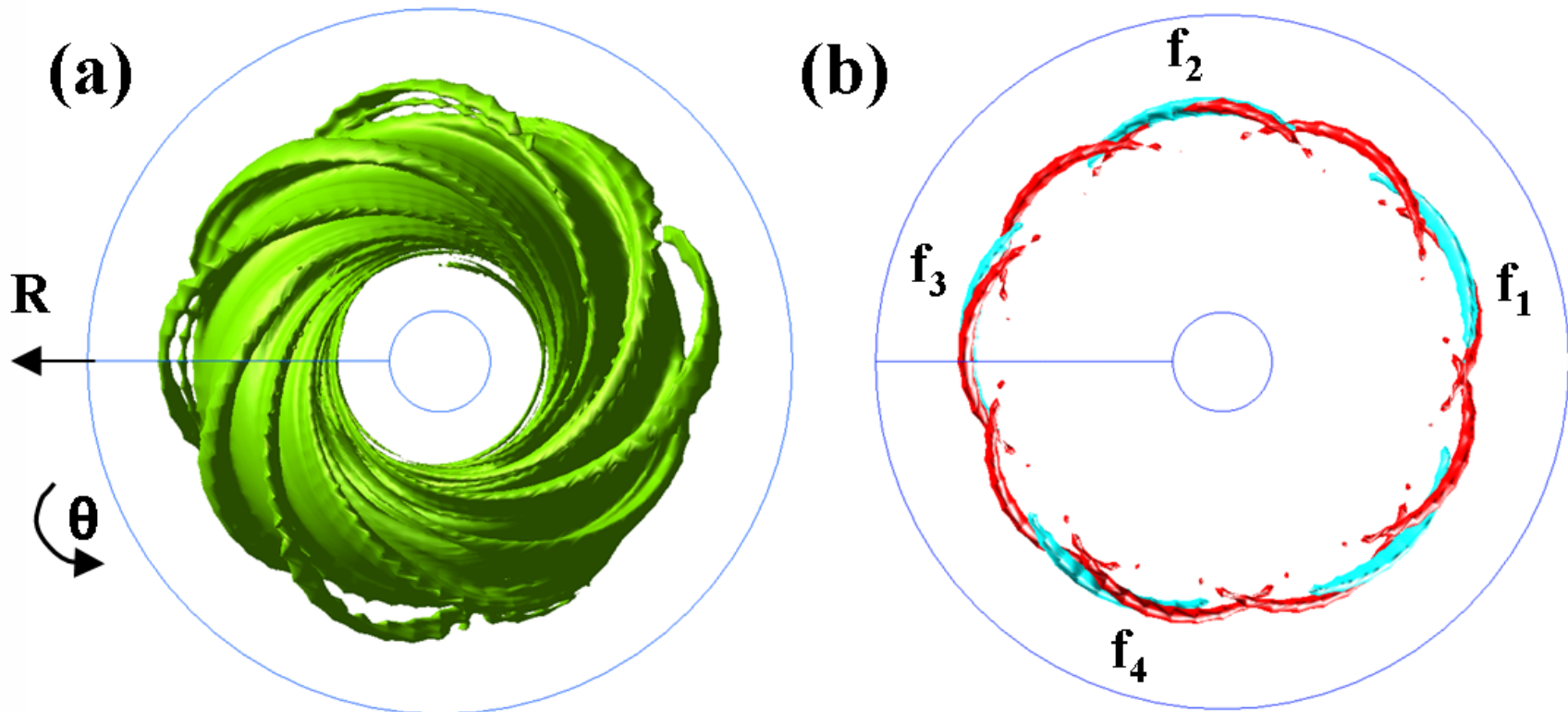
- It's the measure of stability against pressure driven modes for a given magnetic field strength

$$\beta \equiv \frac{p}{B^2/2\mu_0} = \frac{\text{plasma pressure}}{\text{magnetic field pressure}}$$

Non uniform Growth of Filaments

Top view of pressure iso-surface, shows the number of filament are much less then the dominant mode ($n=9$).

Toroidal Coupling of $n=9$ and $n=5$



This occur because of coexistence of multiple modes. The coupling of nonlinear toroidal modes results in the non-uniform growth of the filament.

The Energy Principal

- The energy principle is based on the idea that an equilibrium is unstable if any perturbation of the equilibrium lowers the potential energy.
- The potential energy change due to an arbitrary displacement ξ can be calculated using MHD Eqs and the linear approx.
- The force arising from the displacement ξ follows from the momentum equation:

$$\vec{F}(\vec{\xi}) = \rho \frac{\partial^2 \vec{\xi}}{\partial t^2} = \vec{j}_1 \times \vec{B}_0 + \vec{j}_0 \times \vec{B}_1 - \nabla p_1$$

- The energy change resulting from this displacement of plasma given by the integral

$$\delta W = -\frac{1}{2} \int \vec{\xi} \cdot \vec{F} d\tau$$

$$\delta W < 0 \quad (\text{unstable})$$

$$\delta W > 0 \quad (\text{stable})$$

The Energy Principal

- The energy principle is based on the idea that an equilibrium is unstable if any perturbation of the equilibrium lowers the potential energy.
- The potential energy change due to an arbitrary displacement ξ can be calculated using MHD Eqs and the linear approx.
- The force arising from the displacement ξ follows from the momentum equation:

$$\vec{F}(\vec{\xi}) = \rho \frac{\partial^2 \vec{\xi}}{\partial t^2} = \vec{j}_1 \times \vec{B}_0 + \vec{j}_0 \times \vec{B}_1 - \nabla p_1$$

- The energy change resulting from this displacement of plasma given by the integral

$$\begin{aligned} \delta W = \frac{1}{2} \int_P d^3x & \left[\gamma p |\nabla \cdot \xi|^2 + |Q_\perp|^2 + B^2 |\nabla \cdot \xi_\perp + 2\xi_\perp \cdot \kappa|^2 \right. \\ & - j_\parallel (\xi^* \times b \cdot Q_\perp) \\ & \left. - 2(\xi_\perp \cdot \nabla p)(\xi_\perp^* \cdot \kappa) \right], \end{aligned} \tag{19}$$

Magnetohydrodynamics

$$\frac{d\rho}{dt} = -\rho \vec{\nabla} \cdot \vec{v} \quad (\text{mass conservation})$$

$$\rho \frac{d\vec{v}}{dt} = \vec{j} \times \vec{B} - \nabla p \quad (\text{momentum equation})$$

$$\vec{j} = \vec{\nabla} \times \vec{B} / \mu_0 \quad (\text{Ampere's law})$$

$$\frac{\partial \vec{B}}{\partial t} = -\vec{\nabla} \times \vec{E} \quad (\text{Faraday's law})$$

$$\vec{E} + \vec{v} \times \vec{B} = \eta \vec{j} \quad (\text{Ohm's law})$$

$$\vec{\nabla} \cdot \vec{B} = 0 \quad (\text{absence of magnetic charges})$$

$$\frac{dp}{dt} = -\gamma p \vec{\nabla} \cdot \vec{v} \quad (\text{adiabatic equation})$$

These equations are solved to investigate a plasma equilibrium and the stability of this equilibrium to perturbations.

Ideal MHD Instabilities

- Driving forces for ideal (no dissipation) MHD instabilities:
 - Parallel current density
 - Pressure gradient

Compression magnetic field
fast waves

Bending of magnetic field lines
Alfven waves

Compression of pressure,
sound (slow) waves

$$\delta W = \frac{1}{2} \int dV \left(|B_{1,\perp}|^2 + B_0^2 |\nabla \cdot \xi_{\perp} + 2\xi_{\perp} \cdot \kappa|^2 + \lambda p_0 |\nabla \cdot \xi|^2 \right) - \int dV \left(2(\xi_{\perp} \cdot \nabla p_0)(\kappa \cdot \xi_{\perp}) + J_{0,\parallel} (\xi_{\perp} \times B_0 / B_0) \cdot B_{1,\perp} \right)$$

Pressure gradient
Curvature(K)
Ballooning instability

Parallel current drive
kink instability

Pressure Driven Instabilities

- Mainly driven by the pressure gradient, *i.e.*, modes for which the fourth term has the dominant destabilizing contribution.

$$2(\xi_{\perp} \cdot \nabla p_0)(\kappa \cdot \xi_{\perp})$$

- One sees that this term can be destabilizing when $\xi \cdot \nabla p$ and $\kappa \cdot \xi$ have the same sign, and this effect is strongest when the vectors ∇p and κ are in the same direction (unfavourable curvature).
- Example: Ballooning instability

Ballooning Modes

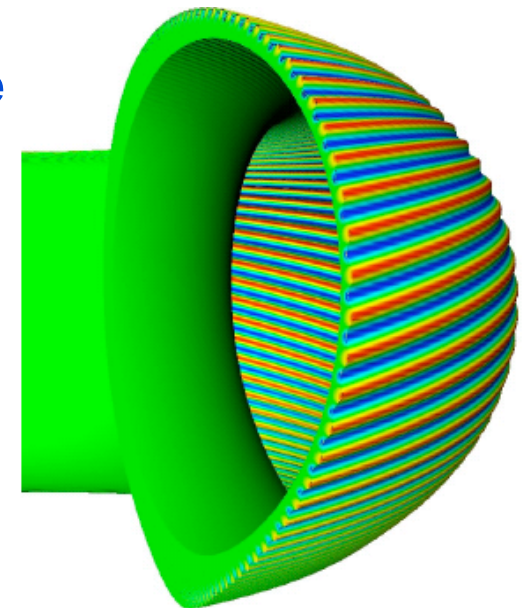
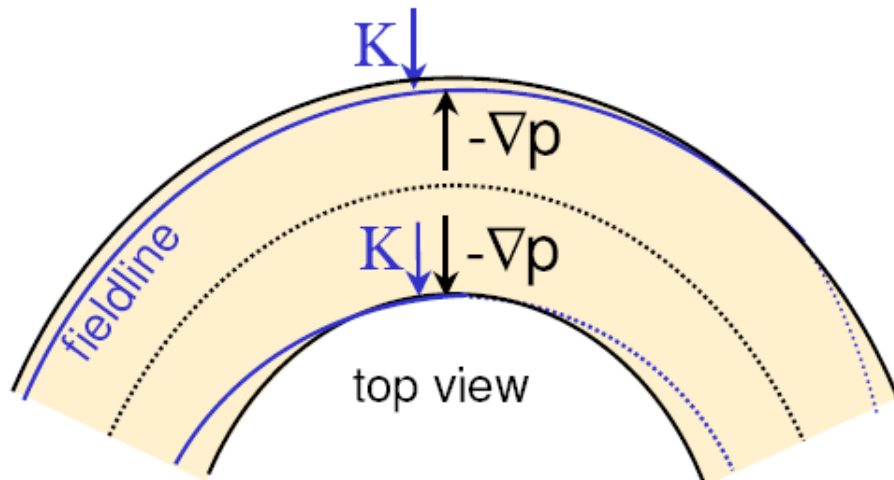
Instability drive: pressure gradient ($-\nabla p$) against curvature (κ)

– Unstable on outside of torus, stabilizing on inside

=> ballooning mode localized on low-field (outer-side) of torus

– radially localized (in high pressure gradient region) to avoid stabilizing bending of magnetic field lines

– High toroidal mode numbers most unstable



n=10 ballooning mode 51

Current Driven Instabilities

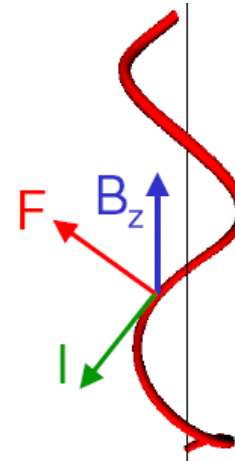
- **Instabilities which are driven by the energy stored in the current parallel to the magnetic field**

$$J_{0,\parallel} (\xi_{\perp} \times B_0 / B_0) \cdot B_{1,\perp}$$

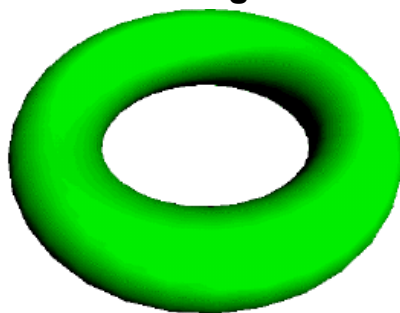
- **The driving force is due to the tendency of two conducting wires (flux tubes) with parallel currents to repel each other.**
- **The destabilizing effect remains even if the plasma pressure is small.**
- **For example: External and internal Kink modes**

External Kink Modes

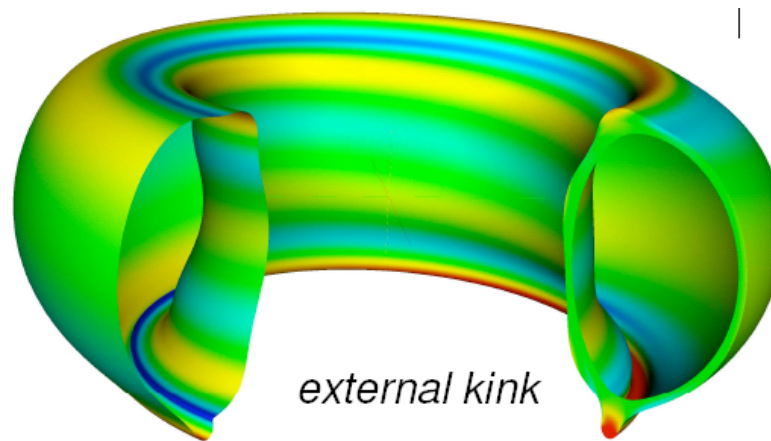
- Simplest model for current driven kink modes is a current carrying wire in a parallel magnetic field
 - unstable to helical deformation
- Ideal MHD kink mode deforms surface
 - driven by parallel current
 - requires a rational q surface just outside plasma
 - Magnetic topology remains the same in ideal MHD



Peeling modes are localised external kink modes driven by the J_{edge}



Cartoon of $n=1/m=3$
kink mode



external kink
instability in JET tokamak

Tearing Modes

- Finite resistivity allows a change of topology of magnetic configuration
 - Tearing modes, driven by current gradients, lead to the formation of magnetic islands on rational q ($=m/n$) surfaces
 - Local flattening of current and pressure profile
 - “Neoclassical” tearing modes are driven by a local pressure gradient
 - absence of the pressure gradient (bootstrap current) inside (existing island) increases island size
- requires a large enough initial perturbation, i.e. by another MHD mode
- can lead to pressure limit below ideal MHD stability limits

